

**Manuscript version: Author's Accepted Manuscript**

The version presented in WRAP is the author's accepted manuscript and may differ from the published version or Version of Record.

**Persistent WRAP URL:**

<http://wrap.warwick.ac.uk/166319>

**How to cite:**

Please refer to published version for the most recent bibliographic citation information. If a published version is known of, the repository item page linked to above, will contain details on accessing it.

**Copyright and reuse:**

The Warwick Research Archive Portal (WRAP) makes this work by researchers of the University of Warwick available open access under the following conditions.

Copyright © and all moral rights to the version of the paper presented here belong to the individual author(s) and/or other copyright owners. To the extent reasonable and practicable the material made available in WRAP has been checked for eligibility before being made available.

Copies of full items can be used for personal research or study, educational, or not-for-profit purposes without prior permission or charge. Provided that the authors, title and full bibliographic details are credited, a hyperlink and/or URL is given for the original metadata page and the content is not changed in any way.

**Publisher's statement:**

Please refer to the repository item page, publisher's statement section, for further information.

For more information, please contact the WRAP Team at: [wrap@warwick.ac.uk](mailto:wrap@warwick.ac.uk).

# Cross-section stability and design of normal strength and high strength steel I-sections in fire

Merih Kucukler

*School of Engineering, University of Warwick, Coventry, CV4 7AL, UK*

---

## Abstract

The structural response and design of normal strength and high strength steel I-sections at elevated temperatures are investigated in this paper. The shell finite element models of steel I-section elements capable of replicating their behaviour in fire are developed and validated against experimental results from the literature. The validated shell finite element models are then utilised to generate extensive structural performance data for steel I-sections, considering a broad range of plate slenderness values for cross-section elements, elevated temperature levels, cross-section aspect ratios as well as different loading conditions and normal strength and high strength steel grades. The accuracy of the existing methods provided in the European structural steel fire design standard EN 1993-1-2 and its upcoming version prEN 1993-1-2 for the ultimate strength predictions of normal strength and high strength steel cross-sections in fire is assessed. Scope for improvement is observed. Considering this, a new method for the ultimate strength predictions of normal strength and high strength steel sections at elevated temperatures is put forward. It is shown that the proposed method leads to more accurate ultimate strength predictions for normal strength and high strength steel I-sections in fire with a higher level of reliability relative to the existing design methods provided in EN 1993-1-2 and prEN 1993-1-2.

*Keywords:* Buckling; Finite element modelling; Fire; Geometric imperfections; I-section; Local buckling; Steel; S460; S690

---

## 1. Introduction

The reductions in strength and stiffness as well as considerably more nonlinear material response of steel at elevated temperatures can lead to substantial decreases in the ultimate strengths of steel sections in fire. In the existing structural steel design standards such as EN 1993-1-2 [1] and AISC 360-16 [2], the reduced ultimate strengths of steel I-sections in fire are typically determined utilising room temperature cross-section design equations in conjunction with reduced material properties of steel at elevated temperatures. However, this approach fails to consider the influence of the significantly more nonlinear stress-strain

---

*Email address:* merih.kucukler@warwick.ac.uk (Merih Kucukler)

response of steel at elevated temperatures on the behaviour, which may require the use of cross-section design equations specifically established for the accurate ultimate resistance predictions of steel sections in fire.

Considering that it may be necessary to develop specific equations for the design of steel sections at elevated temperatures, a number of research studies have been performed on the behaviour and design of steel sections in fire [3–10]. The earlier study of Ranby [3] indicated that the use of the elevated temperature 0.2% proof material strength in conjunction with the room temperature effective width and cross-section design equations provided in the draft version of the European room temperature design standard ENV 1993-1-1 [11] may provide safe estimations for steel sections undergoing local buckling in fire. This approach was adopted in the European structural steel fire design standard EN 1993-1-2 [1]. However, Knobloch and Fontana [4] and Couto et al. [9] observed that EN 1993-1-2 [1] may lead to inaccurate estimations of the ultimate resistances of steel sections at elevated temperatures. Taking into account this inaccuracy, Knobloch and Fontana [4] put forward a strain based design approach for the ultimate resistance predictions of steel sections in fire, while Couto et al. [8, 9] proposed bespoke effective width and cross-section design equations for the ultimate strength estimations of steel sections at elevated temperatures; the effective width and cross-section design equations put forward in Couto et al. [8, 9] will appear in the upcoming version of EN 1993-1-2 [1], which is currently referred to as prEN 1993-1-2 [12]. However, none of the mentioned previous studies [3–10] took into account the behaviour of high strength steel I-sections at elevated temperatures which can be significantly different than that of normal strength steel I-sections owing to considerable differences in their elevated temperature material behaviour. Moreover, the effective width and cross-section design equations proposed in [8, 9] do not take into account the differential erosions of the strength and stiffness of steel at elevated temperatures, which may influence the behaviour of normal strength and high strength steel I-sections in fire.

For the purpose of extensively exploring the behaviour of normal and high strength steel I-sections at elevated temperatures, a comprehensive research study is carried out in this paper. Shell finite element models of normal strength and high strength steel I-section elements are developed and validated against experimental results from the literature. Through the Geometrically and Materially Nonlinear Analyses with Imperfections (GMNIA) of the validated finite element models, extensive structural performance data are generated for the behaviour of steel I-sections in fire, taking into account various plate slendernesses for cross-sections elements, elevated temperature levels, cross-section aspect ratios as well as different loading conditions and grade S690 and S460 high strength steels and grade S355, S275 and S235 normal strength steels. The accuracy and reliability of the effective width and cross-section design equations provided in the European structural steel fire design standard EN 1993-1-2 [1] and its upcoming version prEN 1993-1-2 [12] are assessed, where scope for improvement is observed. Taking into account this, new cross-section design equations employing the effective width formulae developed in Kucukler [13] for normal strength and high strength steel sections are proposed. The higher accuracy and reliability of the proposed cross-section design equations relative to those provided in EN 1993-1-2 [1] and prEN 1993-1-2 [12] are demonstrated for the ultimate strength predictions of normal strength and high

strength steel I-sections at elevated temperatures. It should be noted that in this paper, the elevated temperature behaviour and design of normal and high strength steel I-sections under axial compression and major axis bending are taken into consideration; the behaviour and design of steel I-sections under minor axis bending in fire will be extensively considered in a future study adopting the plastic effective width formulae [14, 15] able to account for the development of partial plasticity in outstand flange elements subjected to stress gradients.

## 2. Finite element modelling

The shell finite element models of steel I-section elements able to replicate their structural response at elevated temperatures are developed in this section. The developed finite element models are used to perform extensive parametric studies on the behaviour of normal strength and high strength steel sections at elevated temperatures. In the following sections, the results from the parametric studies will be used for (i) the assessment of the accuracy of EN 1993-1-2 [1] and prEN 1993-1-2 [12] and (ii) the establishment of a new method for the design of normal strength and high strength steel sections in fire.

### 2.1. Element type and modelling assumptions

The finite element analysis software Abaqus [16] was employed to generate the finite element models. The four-noded reduced integration shell finite element referred to as S4R, which has been used in similar applications [17–22], was utilised to create all the finite element models in this study. To accurately capture the structural response of steel sections in fire, twenty elements were used across each web and flange plate; the number of the elements along the lengths of the modelled I-section steel elements were selected such that the element aspect ratios within the web plates were equal to unity [15, 21]. Note that the member length  $L$  to cross-section depth  $h$  ratios of the modelled I-section elements were equal to 3.0 (i.e.  $L/h = 3.0$ ) to consider the local buckling effects in accordance with [23]. To prevent the overlapping of the flange and web plates, the web plate was offset considering the thickness of the flange plates. Loading was applied to the finite element models as point forces and bending moments at the centroids of the end sections. With the aim of avoiding concentrated plasticity and local buckling in the proximity of the load application points, the nodes at the end sections were coupled to the nodes at the centroids of the end sections through kinematic coupling constraints where the loading was applied. Unless otherwise stated, isothermal analyses of the finite element models were performed in all the considered cases, assuming an initial uniform temperature increase to a predefined temperature value  $\theta$ , which was represented by the modification of the material response, and then applying the loading at the designated elevated temperature level  $\theta$ . To trace the full load-displacement response of the modelled I-section elements which included the post-ultimate behaviour, the modified Riks analysis [24, 25] was used in all the finite element simulations. The adopted element type and modelling assumptions are illustrated in Fig. 1. The description of the elevated temperature material models used for normal and high strength steels and the definition of the geometric imperfections within the finite element models are described in the following subsections.

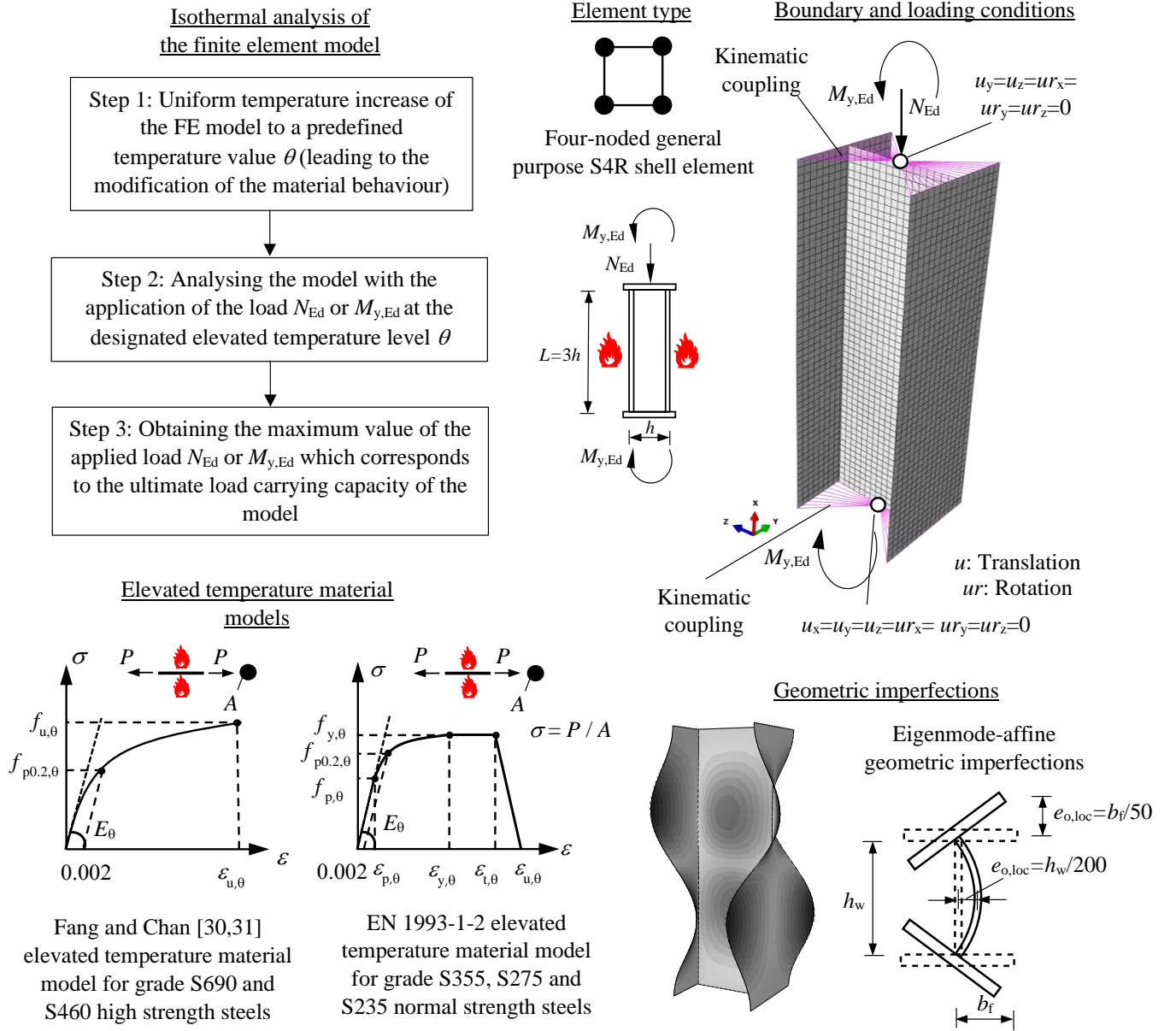


Figure 1: Illustration of the adopted element type and modelling assumptions

## 2.2. Material modelling

To mimic the behaviour of normal strength grade S355, S275 and S235 steel I-sections, the four stage elevated temperature material model provided in EN 1993-1-2 [1] was utilised, whereby the elevated temperature stress versus strain relationship was defined by means of the following equations:

$$\sigma = \epsilon E_{\theta} \quad \text{for} \quad \epsilon \leq \epsilon_{p,\theta},$$

$$\sigma = f_{p,\theta} - c + (b/a) \sqrt{a^2 - (\epsilon_{y,\theta} - \epsilon)^2} \quad \text{for} \quad \epsilon_{p,\theta} \leq \epsilon \leq \epsilon_{y,\theta},$$

$$\begin{aligned} \sigma &= f_{y,\theta} \quad \text{for} \quad \epsilon_{y,\theta} \leq \epsilon \leq \epsilon_{t,\theta}, \\ \sigma &= f_{y,\theta} [1 - (\epsilon - \epsilon_{t,\theta}) / (\epsilon_{u,\theta} - \epsilon_{t,\theta})] \quad \text{for} \quad \epsilon_{t,\theta} \leq \epsilon \leq \epsilon_{u,\theta}, \end{aligned} \quad (1)$$

in which  $\sigma$  and  $\epsilon$  are the engineering stress and strain and  $E_\theta$ ,  $f_{p,\theta}$  and  $f_{y,\theta}$  are the Young's modulus, the proportional limit and the effective yield strength at temperature  $\theta$ , respectively. In eq. (1),  $\epsilon_{p,\theta}$  is the strain at proportional limit calculated as  $\epsilon_{p,\theta} = f_{p,\theta} / E_\theta$ ,  $\epsilon_{y,\theta}$  is the yield strain equal to 0.02 (i.e.  $\epsilon_{y,\theta} = 0.02$ ),  $\epsilon_{t,\theta}$  is the limiting strain for yield strength taken as 0.15 (i.e.  $\epsilon_{t,\theta} = 0.15$ ) and  $\epsilon_{u,\theta}$  is the ultimate strain equal to 0.20 (i.e.  $\epsilon_{u,\theta} = 0.20$ ). The auxiliary coefficients  $a$ ,  $b$  and  $c$  used in eq. (1) are determined as given below:

$$\begin{aligned} a &= \sqrt{(\epsilon_{y,\theta} - \epsilon_{p,\theta})(\epsilon_{y,\theta} - \epsilon_{p,\theta} + c/E_\theta)}, \\ b &= \sqrt{c(\epsilon_{y,\theta} - \epsilon_{p,\theta})E_\theta + c^2}, \\ c &= \frac{(f_{y,\theta} - f_{p,\theta})^2}{(\epsilon_{y,\theta} - \epsilon_{p,\theta})E_\theta - 2(f_{y,\theta} - f_{p,\theta})}. \end{aligned} \quad (2)$$

Fig. 2 (a) shows that the elevated temperature effective yield strength  $f_{y,\theta}$  and proportional

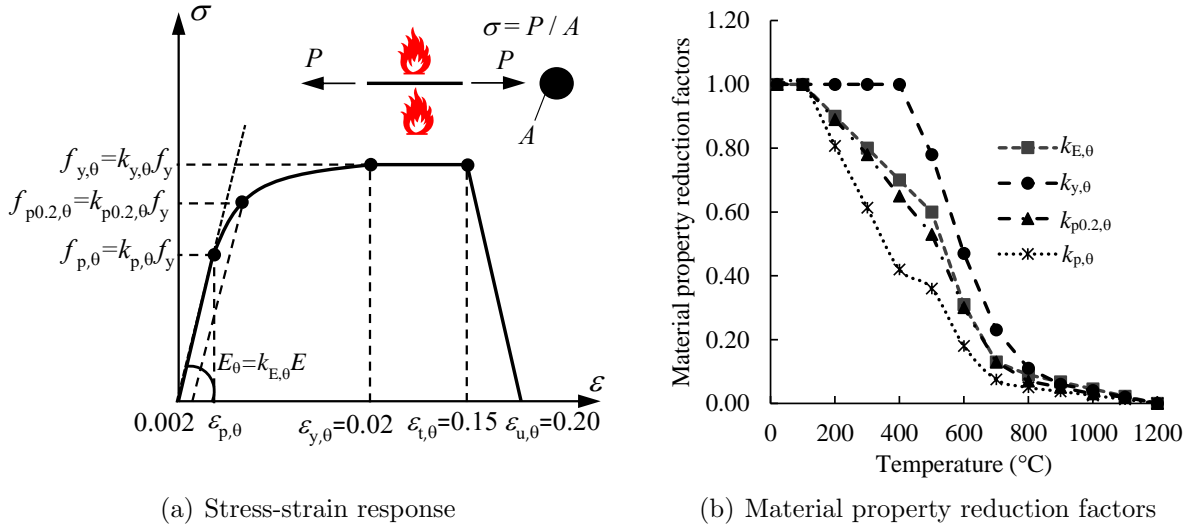


Figure 2: Stress-strain relationship and material property reduction factors for normal strength steel at elevated temperatures adopted in this study as given in [1]

limit  $f_{p,\theta}$  are calculated by multiplying the elevated temperature yield strength reduction factor  $k_{y,\theta}$  and proportional limit reduction factor  $k_{p,\theta}$  by the room temperature yield strength  $f_y$  (i.e.  $f_{y,\theta} = k_{y,\theta} f_y$  and  $f_{p,\theta} = k_{p,\theta} f_y$ ). On the other hand, the elevated temperature Young's modulus  $E_\theta$  is calculated by multiplying the elevated temperature Young's modulus reduction factor  $k_{E,\theta}$  by the room temperature Young's modulus of carbon steel  $E$  (i.e.  $E_\theta = k_{E,\theta} E$ ). In this paper, the values of  $k_{y,\theta}$ ,  $k_{p,\theta}$  and  $k_{E,\theta}$  provided in EN 1993-1-2 [1], which are displayed in Fig. 2 (b), were employed for grade S355, S275 and S235 steels. Note that  $k_{p0.2,\theta}$  is the elevated temperature 0.2% proof strength reduction factor multiplied by

the yield strength  $f_y$  to determine the elevated temperature 0.2% proof strength  $f_{p0.2,\theta}$  (i.e.  $f_{p0.2,\theta} = k_{p0.2,\theta} f_y$ ).

Even though the EN 1993-1-2 [1] elevated temperature material model provides accurate predictions of the elevated temperature stress-strain response of normal strength steels [26], previous research [27–29] showed that it may lead to unconservative estimations of the elevated temperature material response of high strength steels; thus, the use of the EN 1993-1-2 [1] elevated temperature material model to represent the elevated temperature material response of high strength steel I-sections in numerical simulations may result in overestimations of their ultimate resistances. Taking into account this, the EN 1993-1-2 [1] elevated temperature material model was only employed to replicate the behaviour of normal strength grade S355, S275 and S235 steel I-sections in this study. To mimic the behaviour of high strength steel I-sections, the two-stage elevated temperature material model put forward in Fang and Chan [30, 31] for grade S690 and S460 high strength steels, based on the elevated temperature material model recommended in Chen and Young [32], was used. This elevated temperature material model is defined by means of the following equations:

$$\begin{aligned} \epsilon &= \frac{\sigma}{E_\theta} + 0.002 \left( \frac{\sigma}{f_{p0.2,\theta}} \right)^{n_\theta} \quad \text{for } \sigma \leq f_{p0.2,\theta}, \\ \epsilon &= \frac{\sigma - f_{p0.2,\theta}}{E_{p0.2,\theta}} + \epsilon_{u,\theta} \left( \frac{\sigma - f_{p0.2,\theta}}{f_{u,\theta} - f_{p0.2,\theta}} \right)^{m_\theta} + \epsilon_{p0.2,\theta} \\ &\quad \text{for } f_{p0.2,\theta} \leq \sigma \leq f_{u,\theta}, \end{aligned} \quad (3)$$

where  $\epsilon_{p0.2,\theta}$  is the total strain corresponding to  $f_{p0.2,\theta}$ ,  $n_\theta$  and  $m_\theta$  are the exponents defining the roundedness of the stress-strain curve and  $E_{p0.2,\theta}$  is the tangent modulus at  $f_{p0.2,\theta}$ , which is calculated by

$$E_{p0.2,\theta} = \frac{E_\theta}{(1 + 0.002n_\theta E_\theta / f_{p0.2,\theta})}. \quad (4)$$

The exponents  $n_\theta$  and  $m_\theta$  can be determined using the following expressions for grade S690 steel [31]:

$$\begin{aligned} n_\theta &= 7 - \frac{\theta}{250}, \\ m_\theta &= 1.6 + \frac{\theta}{600}, \end{aligned} \quad (5)$$

and the following equations for grade S460 steel [30, 31]:

$$\begin{aligned} n_\theta &= 12 - \frac{\theta}{100}, \\ m_\theta &= 2.1 + \frac{3\theta}{600}. \end{aligned} \quad (6)$$

Note that the elevated temperature model given by eq. (3) was developed in [30–32] considering the two-stage compound Ramberg-Osgood material model proposed by Mirambell and

Real [33] for the representation of the room temperature stress-strain behaviour of stainless steels. In Chen and Young [32] and Fang and Chan [30, 31], it was illustrated that the elevated temperature material stress-strain response of high strength steels can be accurately represented by means of this material model with appropriate  $n_\theta$  and  $m_\theta$  exponents for the representation of the roundedness of the stress-strain curves.

The elevated temperature material properties (i.e.  $E_\theta$ ,  $f_{p0.2,\theta}$ ,  $f_{y,\theta}$ ,  $f_{u,\theta}$  and  $\epsilon_{u,\theta}$ ) of grade S690 and S460 steels were determined using the results from the elevated temperature material tests performed on high strength grade S690 and S460 steels by Qiang et al. [34] and Qiang et al. [35], respectively. The room temperature yield strength  $f_y$ , ultimate tensile strength  $f_u$  and strain  $\epsilon_u$  and the Young's modulus  $E$  for grade S690 and S460 steels obtained from the room temperature material tests in [34, 35] were multiplied by the material reduction factors (i.e.  $k_{E,\theta}$ ,  $k_{p0.2,\theta}$ ,  $k_{y,\theta}$  and  $k_{u,\theta}$ ) established in [34, 35] to determine their values at corresponding elevated temperature levels  $\theta$  in this study, i.e.  $E_\theta = k_{E,\theta}E$ ,  $f_{p0.2,\theta} = k_{p0.2,\theta}f_y$ ,  $f_{y,\theta} = k_{y,\theta}f_y$ ,  $f_{u,\theta} = k_{u,\theta}f_u$  and  $\epsilon_{u,\theta} = k_{\epsilon_{u,\theta}}\epsilon_u$ . Thus, the room temperature material properties of grade S690 steel were taken as  $E = 204690$  MPa,  $f_y=789$  MPa,  $f_u=821$  MPa and  $\epsilon_u=0.051$  as determined in [34], while those of grade S460 steel were taken as  $E = 202812$  MPa,  $f_y=504$  MPa,  $f_u=640$  MPa and  $\epsilon_u=0.115$  as obtained in [35]. The material reduction factors for grade S690 and S460 steels derived in [34, 35] and used in this study and the Ramberg Osgood exponents are provided in Tables 1 and 2 for different elevated temperature values. Comparison of the Young's modulus  $k_{E,\theta}$  and yield strength

Table 1: Material reduction factors derived by Qiang et al. [34] and Ramberg-Osgood exponents used in this study for grade S690 steel ( $E = 204690$  MPa,  $f_y=789$  MPa,  $f_u=821$  MPa and  $\epsilon_u=0.051$ )

Temperature ( $^{\circ}\text{C}$ )	$k_{E,\theta}$	$k_{p0.2,\theta}$	$k_{y,\theta}$	$k_{u,\theta}$	$k_{\epsilon_{u,\theta}}$	$n_\theta$	$m_\theta$
200	0.875	0.884	0.982	0.991	0.957	6.20	1.93
300	0.839	0.879	0.975	0.961	0.696	5.80	2.10
400	0.775	0.794	0.850	0.828	0.280	5.40	2.27
500	0.685	0.628	0.624	0.628	0.161	5.00	2.43
550	0.546	0.554	0.533	0.558	0.178	4.80	2.52
600	0.372	0.380	0.371	0.377	0.196	4.60	2.60
700	0.141	0.100	0.133	0.130	0.333	4.20	2.77

reduction factors  $k_{y,\theta}$  adopted for high strength grade S690 and S460 steels against those adopted for normal strength grade S355, S275 and S235 steels is shown in Fig. 3. It can be seen from the figure that the yield strength reduction factors  $k_{y,\theta}$  for grade S690 and S460 steels are lower than those for normal strength steels, while the Young's modulus reduction is less severe for grade S690 steel but more pronounced for grade S460 steel relative to the Young's modulus reduction rates of normal strength grade S355, S275 and S235 steels. The elevated temperature stress-strain behaviour of grade S690 and S460 steels derived using eq. (3) in conjunction with the elevated temperature material properties obtained from [34, 35] is compared against the elevated temperature stress-strain curves obtained from the material tests of [34, 35] in Fig. 4. As can be seen from the figure, there is a good agreement between



Table 2: Material reduction factors derived by Qiang et al. [35] and Ramberg-Osgood exponents used in this study for grade S460 steel ( $E = 202812$  MPa,  $f_y = 504$  MPa,  $f_u = 640$  MPa and  $\epsilon_u = 0.115$ )

Temperature ( $^{\circ}\text{C}$ )	$k_{E,\theta}$	$k_{p0.2,\theta}$	$k_{y,\theta}$	$k_{u,\theta}$	$k_{\epsilon_u,\theta}$	$n_\theta$	$m_\theta$
200	0.881	0.812	0.994	0.969	0.758	10.00	2.70
300	0.799	0.750	1.000	1.000	0.804	9.00	3.00
400	0.669	0.681	0.949	0.880	0.517	8.00	3.30
500	0.509	0.520	0.739	0.601	0.296	7.00	3.60
550	0.374	0.496	0.559	0.443	0.217	6.50	3.75
600	0.291	0.379	0.415	0.328	0.139	6.00	3.90
700	0.153	0.196	0.187	0.157	0.066	5.00	4.20

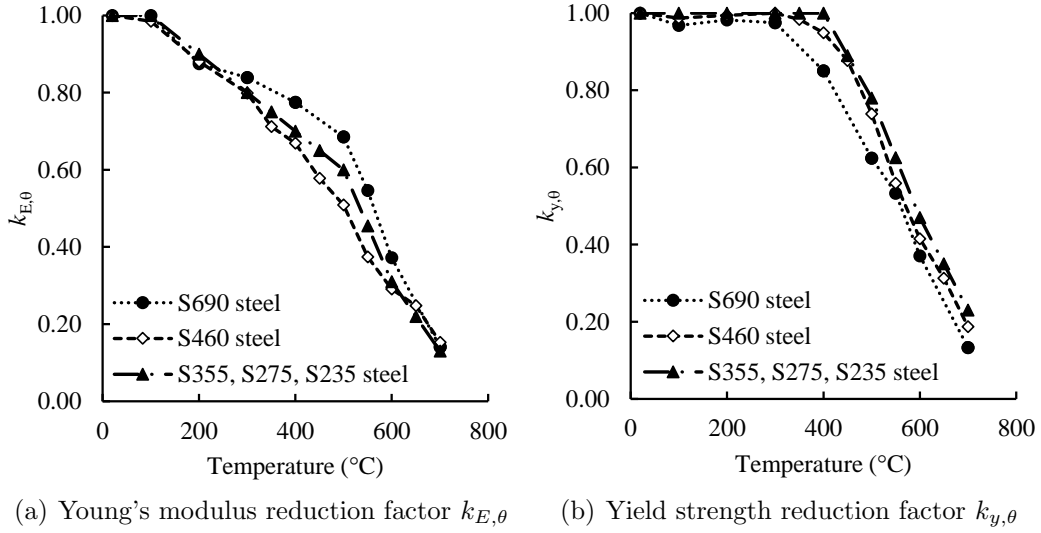
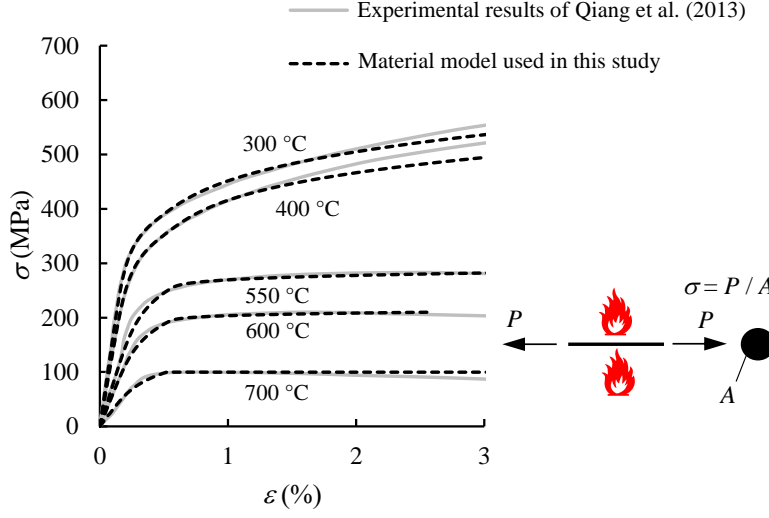


Figure 3: Comparison of the Young's modulus reduction factors  $k_{E,\theta}$  and yield strength reduction factors  $k_{y,\theta}$  for grade S690, S460, S355, S275 and S235 steels adopted in this study

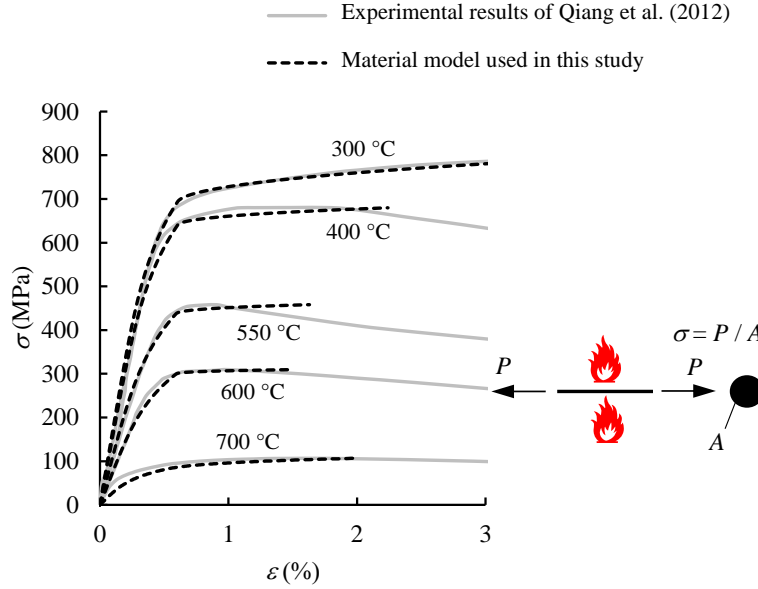
the elevated temperature material stress-strain curves used in the finite element simulations and those obtained from the elevated temperature material tests of [34, 35].

### 2.3. Initial imperfections

To accurately capture the local instability effects in normal strength and high strength steel I-sections at elevated temperatures, local geometric imperfections were incorporated into the finite element models. The shapes of the local geometric imperfections were defined using the shapes of the lowest local buckling modes obtained through the Linear Buckling Analyses (LBA) of the finite element models; the magnitudes of the local geometric imperfections  $e_{o,loc}$  within the modelled I-sections were defined considering the geometric imperfection values recommended in EN 1993-1-5 [36]. In accordance with [36], the lowest local buckling modes from the LBA were scaled to  $1/200$  of the web height  $h_w$  when the largest normalised displacements from the LBA were observed in the web plates (i.e.



(a) S460



(b) S690

Figure 4: Elevated temperature stress-strain response of S690 and S460 grade steels at different elevated temperature levels obtained by [34, 35] and material model adopted in the finite element models

$e_{0,loc} = h_w/200$ ), while the lowest local buckling modes were scaled to  $1/50$  of the half flange width  $b_f$ , when the largest normalised displacements from the LBA occurred in the flange plates (i.e.  $e_{0,loc} = b_f/50$ ).

In Kucukler [13], it is shown that residual stresses have insignificant influence on the local buckling strengths of normal strength and high strength steel plates in fire; Couto et al. [8, 9] and Quiel and Garlock [6] also made similar observations and did not include residual stresses in their numerical studies whose results were used in the development of their effective width

and cross-section design equations. Considering their negligible influence on the ultimate strengths of steel I-sections at elevated temperatures, residual stresses were not incorporated into the finite element models in this paper in accordance with [6, 8, 9, 13].

#### *2.4. Validation of finite element models*

The validation of the finite element modelling approach adopted in this paper was performed using (i) the results from the fire experiments carried out on grade Q235 normal strength and grade Q460 high strength steel welded I-section stub columns by Wang et al. [37] and (ii) those from the fire experiments performed on grade Q690 high strength steel welded I-section stub columns in Sharhan et al. [38]. Note that Q235 is a normal strength steel grade with a standard yield strength of 235 MPa, while Q460 and Q690 are high strength steel grades with standard yield strengths of 460 MPa and 690 MPa, respectively. In the finite element models created for the validation herein, the geometric and material properties and boundary conditions of the specimens reported in [37, 38] were utilised. In accordance with [37, 38], the finite element models were analysed isothermally, where initially, the temperature of a specimen was increased up to a designated value and then the loading was applied up to the failure. The ECCS residual stress pattern [39] was utilised in the finite element models of the grade Q235 normal strength steel welded I-section stub columns, while the residual stress pattern put forward in Bradford and Liu [40] for high strength steel welded I-sections were employed in the finite element models of the grade Q460 and Q690 high strength steel welded I-section stub columns. In addition to the fire tests, the room temperature tests carried out in [37, 38] were also used in the validation of the finite element modelling approach adopted in this paper. Table 3 shows comparison of the ultimate strengths of the specimens observed in the experiments of [37, 38] and those determined through the finite element models created herein. As can be seen from the table, there is a good correlation between the experimental and numerical ultimate resistance values. Note that the discrepancies in the ultimate resistance predictions may result from the differences between the geometric imperfection patterns incorporated into the finite element models as described in Section 2.3 and those of the specimens. Some differences between temperatures measured at different locations of the specimens and reported in the experiments of [37, 38] may also contribute the discrepancies between the numerical and experimental results as uniform temperature distributions were adopted in the numerical models. However, as can be seen in Table 3, the numerical models generally provide ultimate strength values that are in good agreement with those observed in the experiments, indicating their capability of replicating the behaviour of steel I-section stub columns at elevated temperatures. It should be noted that in addition to the validation presented herein, the finite element modelling approach adopted in this paper has also been extensively validated in [15, 20, 41]. Note that in Xing et al. [15] and Kucukler et al. [20], the finite element modelling of the behaviour of stainless steel cross-sections and stainless steel I-section columns in fire was performed, respectively. On the other hand, in Kucukler [41], the finite element modelling of the behaviour of normal and high strength steel circular hollow section columns in fire was carried out. In this paper, different than these previous studies [15, 20, 41], the finite element modelling of the structural response of normal strength and high strength steel I-sections in fire

Table 3: Comparison of the ultimate resistances obtained through the experiments of [37, 38] and those determined through the finite element models created in this study

Study	Cross-section	Steel grade	Critical plate	Temperature (°C)	$N_{u,test}$ (kN)	$N_{u,FE}$ (kN)	$N_{u,FE} / N_{u,test}$
Wang et al. [37]	I-316 × 200 × 6 × 8	Q235	Web	20	1247	1239	0.99
				450	830	798	0.96
				650	280	292	1.04
	I-250 × 250 × 6 × 8	Q235	Flange	20	1375	1290	0.94
				450	930	871	0.94
				650	295	320	1.08
	I-336 × 160 × 8 × 8	Q460	Web	20	2269	2133	0.94
				450	1450	1324	0.91
				650	430	472	1.10
	I-250 × 220 × 8 × 8	Q460	Flange	20	2637	2450	0.93
				450	1650	1484	0.90
				650	430	495	1.15
Sharhan et al. [38]	I-450 × 220 × 12 × 12	Q690	Web	20	7549	6986	0.93
				450	5480	4893	0.89
				600	2245	1896	0.84
	I-400 × 400 × 12 × 12	Q690	Flange	20	8857	8754	0.99
				450	6346	5831	0.92
				600	1960	2260	1.15
							Mean
			COV	0.092			

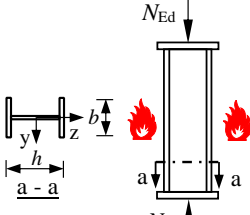
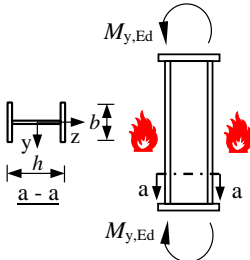
was performed, thereby creating extensive structural performance data on their behaviour.

### 2.5. Parametric studies

Scope of the parametric studies performed in this paper is summarised in Table 4. In the table,  $h$  and  $b$  are the cross-section depth and width and  $\bar{\lambda}_{p,f}$  and  $\bar{\lambda}_{p,w}$  are the plate slendernesses for the flange and web plates, respectively. Note that the plate slenderness  $\bar{\lambda}_p$  of a cross-section element (i.e. flange or web plate) is determined by taking the square root of the ratio of the room temperature material yield strength  $f_y$  to the elastic critical buckling stress  $\sigma_{cr}$  of the corresponding individual cross-section element (i.e.  $\bar{\lambda}_p = \sqrt{f_y/\sigma_{cr}}$ ). In the parametric studies, a total of 14250 steel I-sections with various parameters shown in Table 4 were taken into account, which enabled a comprehensive assessment of the behaviour of normal and high strength steel I-sections at elevated temperatures.

As can be seen from Table 4, the considered normal and high strength I-sections were subjected to pure axial compression and pure major axis bending. The high strength grades of S690 and S460 and the normal strength grades of S355, S275 and S235 were taken into consideration. Five elevated temperature levels were accounted for: 300 °C, 400 °C, 500 °C, 600 °C, 700 °C, while the considered cross-section depth to width ratios ( $h/b$ ) of the I-sections

Table 4: Summary of the parametric studies carried out in this paper

Loading conditions	Steel grades	Temperature	$h/b$	$\bar{\lambda}_{p,w}/\bar{\lambda}_{p,f}$	$\max[\bar{\lambda}_{p,f}, \bar{\lambda}_{p,w}]$
	S690	300 °C	1.00, 2.00, 3.00	0.33,	0.2, 0.3, 0.4, 0.5 0.6, 0.7,
	S460	400 °C		0.67,	0.8, 0.9,
	S355	500 °C		1.00,	1.0, 1.1
	S275	600 °C		1.50,	1.2, 1.3,
	S235	700 °C		3.00	1.4, 1.5,
					1.6, 1.7, 1.8, 1.9, 2.0

were equal to 1.0, 2.0 and 3.0 (i.e.  $h/b = 1.0, 2.0$  and  $3.0$ ). Note that the cross-section width  $b$  was kept constant, which was equal to 200 mm (i.e.  $b = 200$  mm), and the cross-section depth  $h$  was varied to cover the aspect ratios of 1.0, 2.0 and 3.0 in the parametric studies. To investigate the influence of the different ratios between the plate slendernesses of the flange plates and those of the web plates on the behaviour, the web plates slenderness to flange plate slenderness ratios  $\bar{\lambda}_{p,w}/\bar{\lambda}_{p,f}$  of 0.33, 0.67, 1.00, 1.50 and 3.0 (i.e.  $\bar{\lambda}_{p,w}/\bar{\lambda}_{p,f} = 0.33, 0.67, 1.00, 1.50$  and  $3.0$ ) were taken into account, thereby enabling the consideration of both the web-critical and flange-critical cases where the web and flange plates were more susceptible to local buckling effects, respectively. For the purpose of covering the practical range of plate slendernesses encountered in steel I-sections, the largest plate slenderness of a cross-section element (i.e. the largest of the flange and web plate slenderness  $\max[\bar{\lambda}_{p,f}, \bar{\lambda}_{p,w}]$ ) ranged between 0.2 and 2.0 with increment in  $\max[\bar{\lambda}_{p,f}, \bar{\lambda}_{p,w}]$  of 0.1, i.e.  $\max[\bar{\lambda}_{p,f}, \bar{\lambda}_{p,w}] = 0.2-2.0$  with  $\Delta \max[\bar{\lambda}_{p,f}, \bar{\lambda}_{p,w}] = 0.1$ . The results from the parametric studies will be utilised in the following sections for (i) the assessment of EN 1993-1-2 [1] and prEN 1993-1-2 [12] in the predictions of the ultimate resistances of normal and high strength steel I-sections in fire and (ii) the establishment of new cross-section design rules providing accurate, safe and reliable estimations of the cross-section resistances of normal and high strength steel I-sections at elevated temperatures.

### 3. EN 1993-1-2 and prEN1993-1-2 design methods for the ultimate strength predictions of steel I-sections in fire

This sections briefly introduces the rules provided in the European structural steel design standard EN 1993-1-2 [1] and its upcoming version prEN 1993-1-2 [12] for the design of steel

sections in fire. Following the brief introduction of the fire design rules of EN 1993-1-2 [1] and prEN 1993-1-2 [12], their accuracy is assessed for the ultimate strength predictions of normal and high strength steel I-sections at elevated temperatures.

### 3.1. Cross-section classification

EN 1993-1-2 [1] and prEN 1993-1-2 [12] recommend the classification of steel I-sections at elevated temperatures by means of the same cross-section classification rules provided in the European room temperature structural steel design standard EN 1993-1-1 [42] and its upcoming version prEN 1993-1-1 [43] respectively, using a reduced material factor  $\epsilon_\theta$  which is referred to herein as the elevated temperature material factor. The elevated temperature material factor  $\epsilon_\theta$  is determined through the room temperature material factor  $\epsilon$  as

$$\epsilon_\theta = 0.85\epsilon = 0.85\sqrt{235/f_y} \quad \text{where } f_y \text{ in MPa.} \quad (7)$$

In EN 1993-1-1 [42] and prEN 1993-1-1 [43], steel sections are grouped into four classes, where the cross-section class is assumed as the highest class of its constituent plates. The limit width-to-thickness ratios used to specify the classes of the internal and outstand elements of cross-sections are provided in Table 5.

Table 5: The limit width-to-thickness ratios for the classification of cross-section elements at room temperature according to EN 1993-1-1 [42] and prEN 1993-1-1 [43]

Cross-section element	EN 1993-1-1			prEN 1993-1-1		
	Class 1	Class 2	Class 3	Class 1	Class 2	Class 3
Internal element under compression	33 $\epsilon$	38 $\epsilon$	42 $\epsilon$	28 $\epsilon$	34 $\epsilon$	38 $\epsilon$
Internal element under bending	72 $\epsilon$	83 $\epsilon$	124 $\epsilon$	72 $\epsilon$	83 $\epsilon$	121 $\epsilon$
Outstand element under compression	9 $\epsilon$	10 $\epsilon$	14 $\epsilon$	9 $\epsilon$	10 $\epsilon$	14 $\epsilon$

It should be noted that 0.85 reduction factor applied to the room temperature material factor  $\epsilon$  to determine the elevated temperature material factor  $\epsilon_\theta$  in eq. (7) is utilised with the aim of approximating the values of the square root of the ratios of the stiffness reduction factors  $k_{E,\theta}$  to the yield strength reduction factors  $k_{y,\theta}$  (i.e.  $\sqrt{k_{E,\theta}/k_{y,\theta}}$ ) as displayed in Fig. 5, i.e.  $\sqrt{k_{E,\theta}/k_{y,\theta}} \approx 0.85$  and  $\epsilon_\theta = \left(\sqrt{k_{E,\theta}/k_{y,\theta}}\right)\epsilon \approx 0.85\epsilon$ . However, Fig. 5 shows that 0.85 factor may not be very accurate in approximating the values of  $\sqrt{k_{E,\theta}/k_{y,\theta}}$  for high strength steel grade of S690. It should also be emphasised that this type of cross-section classification method adopted in EN 1993-1-2 [1] and prEN 1993-1-2 [12] does not account for the differential erosions of strength and stiffness of steel in fire, which may have a significant effect on the behaviour of steel members at elevated temperatures.

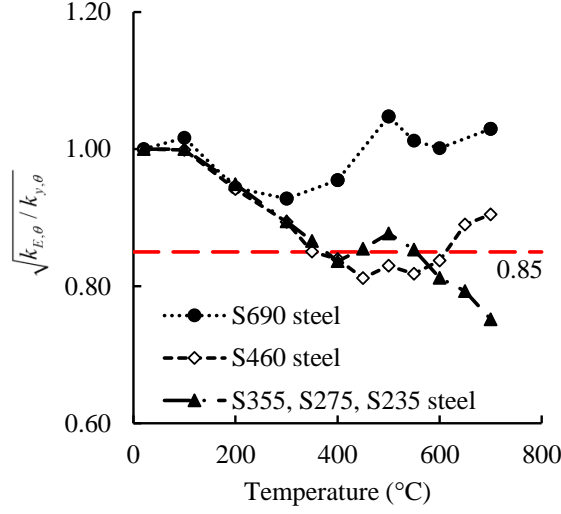


Figure 5: Variation of  $\sqrt{k_{E,\theta}/k_{y,\theta}}$  at different elevated temperature levels for high strength and normal strength steels

### 3.2. Effective width method

According to EN 1993-1-2 [1], the effective cross-section properties of Class 4 sections should be calculated through the room temperature effective width design equations provided in the European steel design standard for plated structures EN 1993-1-5 [36] using the room temperature material factor  $\epsilon$ . Thus, EN 1993-1-2 [1] recommends the use of the effective cross-section properties of steel sections in fire the same as their effective section properties at room temperature. Following equations are provided in EN 1993-1-5 [36] for the determination of the plate buckling reduction factor  $\rho$  of internal steel elements (i.e. webs of steel I-sections):

$$\rho = 1.0 \quad \text{for} \quad \bar{\lambda}_p \leq 0.5 + \sqrt{0.085 - 0.055\psi},$$

$$\rho = \frac{\bar{\lambda}_p - 0.055(3 + \psi)}{\bar{\lambda}_p^2} \leq 1.0 \quad \text{for} \quad \bar{\lambda}_p > 0.5 + \sqrt{0.085 - 0.055\psi}, \quad (8)$$

where  $\psi$  is the ratio of the stresses at the edges of the plate. The expressions for the determination of the plate reduction factor  $\rho$  for outstand elements (i.e. flanges of steel I-sections) given in EN 1993-1-5 [36] are as follows:

$$\rho = 1.0 \quad \text{for} \quad \bar{\lambda}_p \leq 0.748,$$

$$\rho = \frac{\bar{\lambda}_p - 0.188}{\bar{\lambda}_p^2} \quad \bar{\lambda}_p > 0.748. \quad (9)$$

In eqs. (8) and (9), the non-dimensional plate slenderness  $\bar{\lambda}_p$  is determined as:

$$\bar{\lambda}_p = \sqrt{\frac{f_y}{\sigma_{cr}}} = \frac{b/t}{28.4\epsilon\sqrt{k_\sigma}}, \quad (10)$$

in which  $\sigma_{cr}$  is the elastic critical buckling stress of the steel plate,  $b$  and  $t$  are the plate width and thickness and  $k_\sigma$  is the plate buckling coefficient given in EN 1993-1-5 [36] which is dependent on the boundary and loading conditions of the plate. Note that the effective widths  $b_{eff}$  of steel plates are determined by multiplying the plate widths  $b$  by plate buckling coefficients  $\rho$  (i.e.  $b_{eff} = \rho b$ ) following the procedure set out in EN 1993-1-5 [36] for the determination of the effective section properties of steel sections.

In contrast with EN 1993-1-2 [1], the upcoming version of the European structural steel fire design standard prEN 1993-1-2 [12] does not direct the designer to the room temperature steel design standard EN 1993-1-5 [36] but recommends the following expressions for the determination of plate buckling reduction factors  $\rho$

$$\rho = \frac{(\bar{\lambda}_p + 0.9 - 0.26/\epsilon)^{1.5} - 0.055(3 + \psi)}{(\bar{\lambda}_p + 0.9 - 0.26/\epsilon)^3} \leq 1.0, \quad (11)$$

for internal elements and

$$\rho = \frac{(\bar{\lambda}_p + 1.1 - 0.52/\epsilon)^{1.2} - 0.188}{(\bar{\lambda}_p + 1.1 - 0.52/\epsilon)^{2.4}} \leq 1.0, \quad (12)$$

for outstand elements in which  $\epsilon$  is the material factor  $\epsilon = \sqrt{235/f_y}$  as indicated previously. As can be seen from eqs. (8)-(12), the effective width equations of both EN 1993-1-2 [1] and prEN 1993-1-2 [12] do not take into consideration the differential erosions of the strength and stiffness of steel at elevated temperatures, adopting the room temperature plate slendernesses  $\bar{\lambda}_p$  to calculate the effective cross-section properties and ultimate resistances of steel sections in fire.

### 3.3. Cross-section resistance

In both EN 1993-1-2 [1] and prEN 1993-1-2 [43], the ultimate resistance of a steel section is determined taking into account its cross-section class as shown in Table 6 where  $N_{fi,t,Rd}$

Table 6: Cross-section resistances of Class 1, 2, 3 and 4 sections in fire according to EN 1993-1-1 [42] and prEN 1993-1-1 [43]

Cross-section class	Design resistance under compression $N_{fi,t,Rd}$		Design resistance under bending $M_{fi,t,Rd}$	
	EN 1993-1-2	prEN 1993-1-2	EN 1993-1-2	prEN 1993-1-2
Class 1 & 2	$Ak_{y,\theta}f_y/\gamma_{M,fi}$	$Ak_{y,\theta}f_y/\gamma_{M,fi}$	$W_{pl}k_{y,\theta}f_y/\gamma_{M,fi}$	$W_{pl}k_{y,\theta}f_y/\gamma_{M,fi}$
Class 3	$Ak_{y,\theta}f_y/\gamma_{M,fi}$	$Ak_{y,\theta}f_y/\gamma_{M,fi}$	$W_{el}k_{y,\theta}f_y/\gamma_{M,fi}$	$W_{el}k_{y,\theta}f_y/\gamma_{M,fi}$
Class 4	$A_{eff}k_{p0.2,\theta}f_y/\gamma_{M,fi}$	$A_{eff}k_{y,\theta}f_y/\gamma_{M,fi}$	$W_{eff}k_{p0.2,\theta}f_y/\gamma_{M,fi}$	$W_{eff}k_{y,\theta}f_y/\gamma_{M,fi}$

and  $M_{fi,t,Rd}$  are the axial force and bending moment design resistances in fire at time  $t$ ,  $A$



and  $A_{eff}$  are the gross and effective cross-section areas,  $W_{pl}$ ,  $W_{el}$  and  $W_{eff}$  are the plastic, elastic and effective section moduli respectively and  $\gamma_{M,fi}$  is the partial factor for fire design. Table 6 shows that both EN 1993-1-2 [1] and prEN 1993-1-2 [12] adopt the procedure set out in the European room temperature structural steel design standards EN 1993-1-1 [42] and prEN 1993-1-1 [43] for the determination of ultimate resistances of steel sections falling into different cross-section classes by employing the elevated temperature material strengths (i.e.  $f_{y,\theta} = k_{y,\theta}f_y$  and  $f_{p0.2,\theta} = k_{p0.2,\theta}f_y$ ). It should however be noted that while EN 1993-1-2 [1] uses the elevated temperature 0.2% proof strength  $f_{p0.2,\theta} = k_{p0.2,\theta}f_y$  for the determination of the fire resistances of Class 4 sections, prEN 1993-1-2 [12] recommends the determination of the ultimate resistance of Class 4 sections in fire employing the elevated temperature material strength at 2% total strain  $f_{y,\theta} = k_{y,\theta}f_y$ .

### 3.4. Assessment of existing design rules in EN 1993-1-2 and prEN 1993-1-2 for the design of normal and high strength steel I-sections in fire

In Fig. 6, the accuracy of EN 1993-1-2 [1] and prEN 1993-1-2 [12] for the ultimate strength predictions of grade S355 and S235 normal strength and grade S690 and S460 high strength steel I-sections under axial compression in fire is assessed, considering a series of cross-section slendernesses  $\bar{\lambda}_{cs}$ , cross-section aspect ratios  $h/b$  and web plate slenderness to flange plate slenderness ratios  $\bar{\lambda}_{p,w}/\bar{\lambda}_{p,f}$ . As can be seen from the figure, EN 1993-1-2 [1] provides rather inaccurate estimations of the load carrying capacities of normal strength steel I-sections subjected to axial compression at elevated temperatures. Note that the multiple buckling curves and the abrupt changes in the ultimate strength predictions for EN 1993-1-2 [1] at the transitions between Class 3 and Class 4 sections stem from its recommendation of (i) the use of the elevated temperature 0.2% proof strength  $f_{p0.2,\theta}$  for the ultimate strength predictions of Class 4 cross-sections and (ii) the use of the elevated temperature material strength at 2% total strain  $f_{y,\theta}$  for Class 1, 2 and 3 sections. Fig. 6 shows that relative to EN 1993-1-2 [1], the ultimate strength predictions of prEN 1993-1-2 [12] are more accurate for normal strength steel I-sections in fire. Particularly, for the case of the grade S355 steel I-sections shown in Fig. 6 where the ratio of the web plate slenderness  $\bar{\lambda}_{p,w}$  to the flange plate slenderness  $\bar{\lambda}_{p,f}$  is equal to 1.5 (i.e.  $\bar{\lambda}_{p,w}/\bar{\lambda}_{p,f} = 1.5$ ), prEN 1993-1-2 [12] leads to considerably more accurate results relative to EN 1993-1-2 [1] which can be attributed to (i) the adoption of new effective width design equations developed considering the behaviour of steel plates at elevated temperatures in lieu of using the room temperature effective width design equations as recommended in EN 1993-1-2 [1] as well as (ii) the use of the elevated temperature material strengths at 2% total strain  $f_{y,\theta}$  in lieu of the elevated temperature 0.2% proof strengths  $f_{p0.2,\theta}$  for the ultimate strength predictions of Class 4 sections. It should be noted that there are also abrupt changes in the ultimate strength predictions of prEN 1993-1-2 [12] at the transitions between Class 3 and Class 4 sections as can be seen from Fig. 6; the reasons behind these discontinuities of prEN 1993-1-2 [12] ultimate resistance predictions were discussed in detail in Kucukler [13] where it is shown that there exists an incompatibility between the cross-section classification limits and the effective width design equations of prEN 1993-1-2 [1], i.e. it is shown in Kucukler [13] that prEN 1993-1-2 [1]

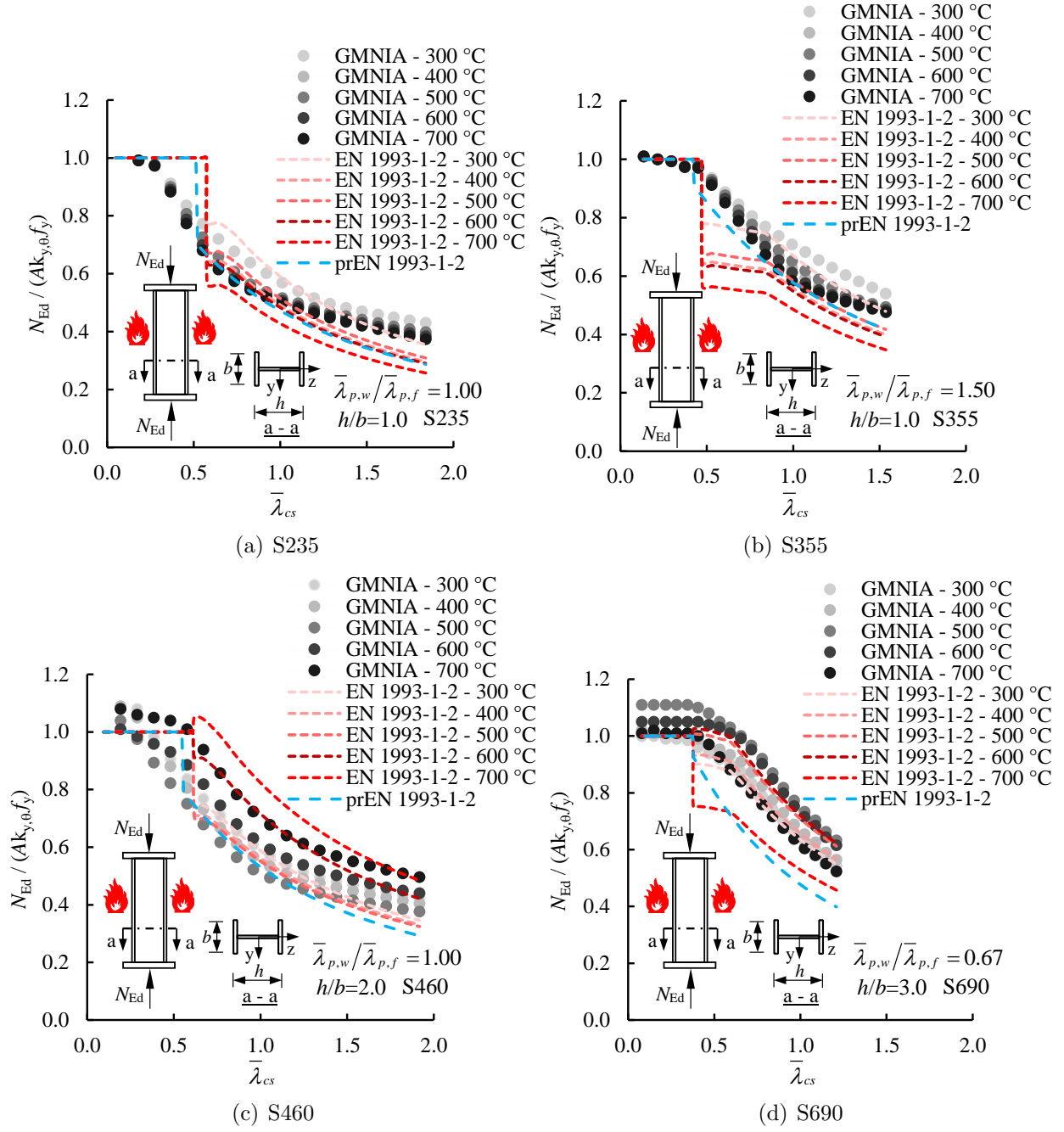


Figure 6: Accuracy of EN 1993-1-2 [1] and prEN 1993-1-2 [12] for the predictions of the ultimate resistances of normal and high strength steel I-sections under compression in fire

effective width design equations provide local plate buckling reduction factors  $\rho$  smaller than 1.0 (i.e.  $\rho < 1.0$ ) for non-Class 4 plates.

Similar to the results observed for normal strength steel I-sections, EN 1993-1-2 [1] also leads to somewhat inaccurate ultimate strength predictions for high strength steel I-sections

at elevated temperatures as displayed in Fig. 6. It is worth noting that relative to the cross-section resistances of normal strength steel I-sections in fire, there is a significantly higher level of scatter in the ultimate resistances of high strength steel I-sections at elevated temperatures as can be seen in Fig. 6. This higher level of scatter in the ultimate resistances of high strength steel I-sections at elevated temperatures, which was also observed in [41] for high strength steel CHS members in fire, was ascribed to (i) the variation of the roundedness of the elevated temperature stress-strain curves of grade S690 and S460 high strength steels at different elevated temperature levels which is represented by means of the varying  $n_\theta$  and  $m_\theta$  Ramberg-Osgood exponents in the definition of the material response as discussed in Section 2.2, (ii) somewhat considerably varying ratios of the elevated temperature 0.2% proof strengths  $f_{p0.2,\theta} = k_{p0.2,\theta} f_y$  to the ultimate strengths  $f_{u,\theta} = k_{u,\theta} f_u$  (i.e.  $f_{p0.2,\theta}/f_{u,\theta}$ ) which can be closer to unity in some cases (see Fig. 4); since high-strength steel I-sections lose their initial elevated temperature stiffness at later stages of the loading history for high  $f_{p0.2,\theta}/f_{u,\theta}$  ratios, the high  $f_{p0.2,\theta}/f_{u,\theta}$  ratios result in higher ultimate cross-section resistances, and (iii) the utilisation of the elevated temperature material strengths at 2% total strain  $f_{y,\theta} = k_{y,\theta} f_y$  in the normalisation of the ultimate resistances even though the elevated temperature material strengths at 2% total strain  $f_{y,\theta} = k_{y,\theta} f_y$  can be on the descending branches of the elevated temperature stress-strain curves of high strength steels due to their lower ductility as shown in Fig. 4. This highlights that, in some cases, the use of the elevated temperature material strengths at 2% total strain  $f_{y,\theta} = k_{y,\theta} f_y$  may not be appropriate for the ultimate strength predictions of high strength steel I-sections in fire. The inappropriateness of the use of the elevated temperature material strengths at 2% total strain  $f_{y,\theta} = k_{y,\theta} f_y$  for the ultimate resistance predictions of high strength steel I-sections in these cases is due to the fact that the behaviour and ultimate resistances of high strength steel I-sections in fire are primarily influenced by the parts of the elevated temperature stress-strain curves up to the elevated temperature ultimate tensile strengths  $f_{u,\theta} = k_{u,\theta} f_u$ . As can be seen from Fig. 6 (c) and (d), there are also sudden increases in the ultimate resistance estimations of EN 1993-1-2 [1] at the transitions from Class 3 to Class 4 sections for high strength steel I-sections in some instances; these result from the adoption of the elevated temperature 0.2% proof strengths  $f_{p0.2,\theta} = k_{p0.2,\theta} f_y$  for the ultimate strength predictions of Class 4 sections, which are greater than the elevated temperature material strengths at 2% total strain  $f_{y,\theta} = k_{y,\theta} f_y$  at some elevated temperature levels for high strength grade S690 and S460 steels due to their low ductility (see Tables 1 and 2 and Fig. 4). Of course, these sudden increases in the strength estimations at the transitions from Class 3 to Class 4 sections do not reflect the physical response accurately as can be seen in Fig. 6 (c) and (d) and again highlight the inappropriateness of the use of the elevated temperature material strengths at 2% total strains  $f_{y,\theta} = k_{y,\theta} f_y$  for the fire design of high strength steel elements in some instances. Relative to EN 1993-1-2 [1], prEN 1993-1-2 [12] leads to safer ultimate strength predictions for high strength steel I-sections in fire as can be seen in Fig. 6 (c) and (d), though the ultimate strength predictions of prEN 1993-1-2 [12] are overly conservative for some cases, which leads to uneconomic designs.

Fig. 7 shows the accuracy of EN 1993-1-2 [1] and prEN 1993-1-2 [12] for the ultimate strength predictions of normal and high strength steel I-sections under bending in fire. Note

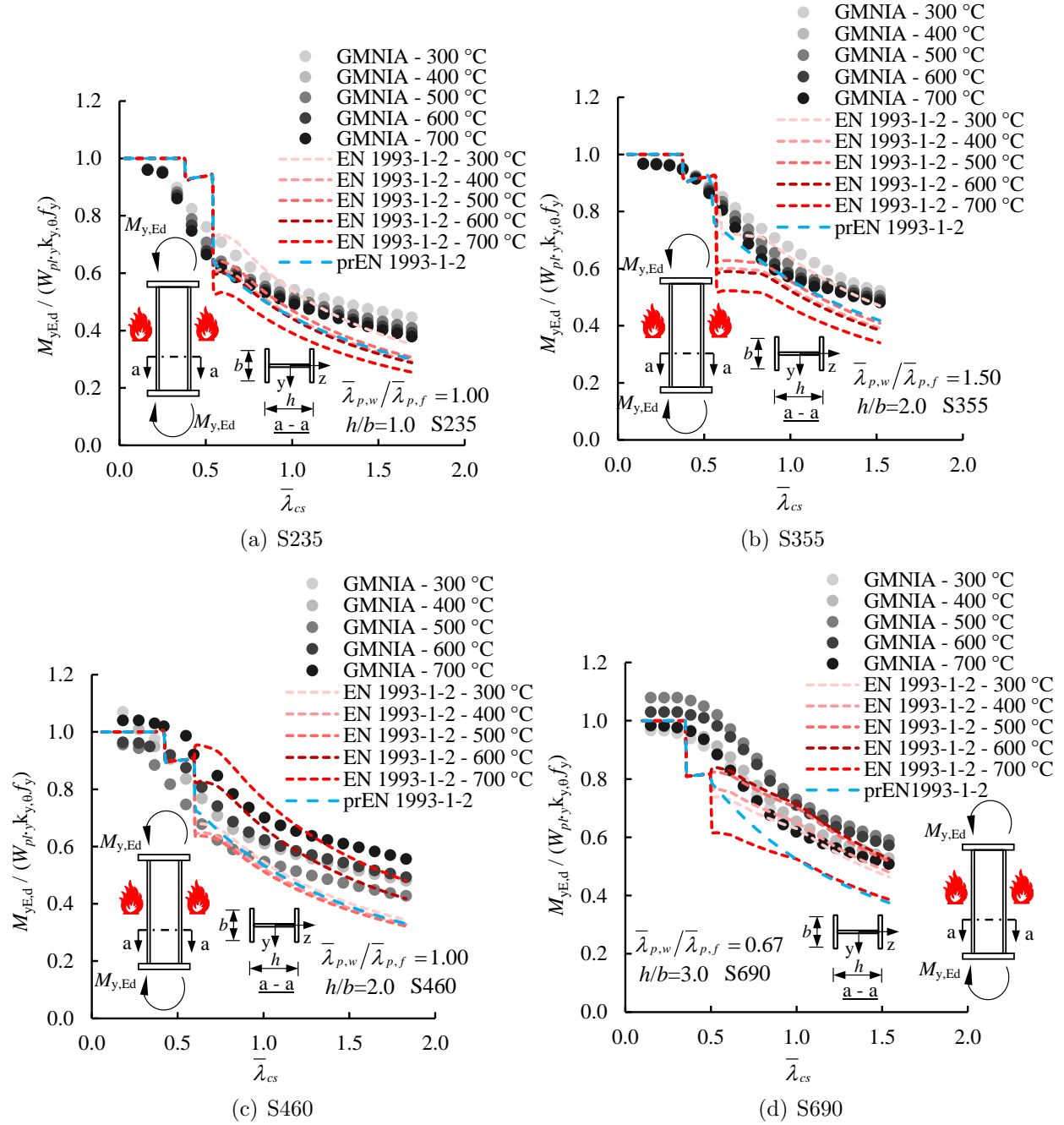


Figure 7: Accuracy of EN 1993-1-2 [1] and prEN 1993-1-2 [12] for the predictions of the ultimate resistances of normal and high strength steel I-sections under bending in fire

that the abrupt steps for EN 1993-1-2 [1] stem from the determination of the ultimate resistances by means of (i) the plastic section moduli for Class 1 and 2 sections, (ii) the elastic section moduli  $W_{el}$  for Class 3 sections and (iii) the elevated temperature 0.2% proof strengths  $f_{p0.2,\theta}$  for Class 4 sections. On the other hand, the sharp changes observed for

prEN 1993-1-2 [12] result from (i) the use of the plastic moduli for Class 1 and 2 sections, (ii) the elastic section moduli  $W_{el}$  for Class 3 sections in the ultimate strength estimations as well as (iii) the incompatibility of the cross-section classification limits of prEN 1993-1-2 [12] with its effective width design equations as discussed previously, which was also addressed in detail in Kucukler [13]. As can be seen from Fig. 7, EN 1993-1-2 [1] leads to somewhat inaccurate results for the ultimate strength estimations of normal and high strength steel I-sections in bending at elevated temperatures. Relative to EN 1993-1-2 [1], prEN 1993-1-2 [12] provides more accurate results, though prEN 1993-1-2 [12] leads to overly conservative ultimate strength predictions for high strength steel I-sections in fire.

The results presented in this subsection indicate that there is scope for improvement of the accuracy of EN 1993-1-2 [1] and prEN 1993-1-2 [12] in the ultimate strength estimations of normal and high strength steel I-sections in fire. There also exist some abrupt changes in the ultimate strength predictions of EN 1993-1-2 [1] and prEN 1993-1-2 [12] which fail to represent the physical response accurately. With the aim of achieving more accurate and consistent predictions of the ultimate resistances of steel I-sections at elevated temperatures, new fire design rules are proposed in this paper for normal and high strength steel sections which are presented in the following section.

#### 4. New design proposals for steel cross-sections in fire

In this section, new design rules based on the recommendations of Kucukler [13] on the local buckling assessment of normal and high strength steel plates in fire are proposed for the ultimate strength predictions of normal and high strength steel I-sections at elevated temperatures. The assessment of the proposed design rules against benchmark results from the GMNIA and EN 1993-1-2 [1] and prEN 1993-1-2 [12] are presented in the following section, considering the broad range of parameters set out in Section 4.

##### 4.1. Cross-section classification

In accordance with Kucukler [13], this paper proposes to replace the traditional four cross-section classes used for room temperature structural steel design with two cross-section classes which are referred to as ‘non-slender’ and ‘slender’ in the determination of the ultimate resistances of steel sections in fire. According to this approach, a cross-section is classified through taking into account the classes of its each constituent cross-section element (i.e. each flange and web plate of an I-section). A class of a cross-section element is determined by comparing its elevated temperature plate slenderness  $\bar{\lambda}_{p,\theta}$  against the plateau plate slendernesses  $\bar{\lambda}_{p,\theta,0}$  given by eq. (14) for internal elements and the plateau plate slendernesses  $\bar{\lambda}_{p,\theta,0}$  given by eq. (16) for outstand elements. If the plate slenderness  $\bar{\lambda}_{p,\theta}$  of a cross-section element is less than or equal to the threshold slenderness  $\bar{\lambda}_{p,\theta,0}$  (i.e.  $\bar{\lambda}_{p,\theta} \leq \bar{\lambda}_{p,\theta,0}$ ), it is classified as ‘non-slender’; on the other hand, if the plate slenderness  $\bar{\lambda}_{p,\theta}$  of a cross-section element is greater than the threshold slenderness  $\bar{\lambda}_{p,\theta,0}$  (i.e.  $\bar{\lambda}_{p,\theta} > \bar{\lambda}_{p,\theta,0}$ ), it is classified as ‘slender’. For a cross-section to be classified as ‘non-slender’, all of its constituent cross-section elements should be classified as ‘non-slender’. If one or more than constituent element of a cross-section is classified as ‘slender’, the cross-section is classified as ‘slender’. Note that

this type of a cross-section classification approach is also recommended in Xing et al. [15, 22] for the fire design of stainless steel sections, which will be adopted in the upcoming version of the European structural steel fire design standard prEN 1993-1-2 [1].

#### 4.2. Effective width method

For the purpose of taking into consideration the differential erosions of the strength and stiffness of steel on the behaviour of steel sections, it is proposed to adopt the elevated temperature plate slenderness  $\bar{\lambda}_{p,\theta}$  in the proposed effective width equations which were developed and extensively validated in Kucukler [13] for the ultimate strength predictions of normal and high strength steel plates in fire.

The following equations are proposed for the determination of the local buckling reduction factor  $\rho$  of both normal and high strength steel internal elements:

$$\rho = \begin{cases} 1.0 & \text{for } \bar{\lambda}_{p,\theta} \leq \bar{\lambda}_{p,\theta,0}, \\ \frac{0.9 - 0.38\epsilon}{\bar{\lambda}_{p,\theta}^{0.85}} - \frac{0.015(3 + \psi)}{\bar{\lambda}_{p,\theta}^{1.7}} & \text{for } \bar{\lambda}_{p,\theta} > \bar{\lambda}_{p,\theta,0} \end{cases} \quad (13)$$

with

$$\bar{\lambda}_{p,\theta,0} = \left( 0.45 - 0.19\epsilon + \sqrt{\frac{(0.9 - 0.38\epsilon)^2}{4} - 0.015(3 + \psi)} \right)^{1.18}, \quad (14)$$

in which  $\psi$  is the ratio between the stresses at the edges of the plate as described in EN 1993-1-5 [36] and  $\epsilon$  is the material factor equal to  $\epsilon = \sqrt{235/f_y}$ .

The plate buckling reduction factors  $\rho$  for outstand elements are calculated as follows:

$$\rho = \begin{cases} 1.0 & \text{for } \bar{\lambda}_{p,\theta} \leq \bar{\lambda}_{p,\theta,0}, \\ \frac{0.9 - 0.3\epsilon}{\bar{\lambda}_{p,\theta}^{0.6}} - \frac{0.05}{\bar{\lambda}_{p,\theta}^{1.2}} & \text{for } \bar{\lambda}_{p,\theta} > \bar{\lambda}_{p,\theta,0} \end{cases} \quad (15)$$

with

$$\bar{\lambda}_{p,\theta,0} = \left( 0.45 - 0.15\epsilon + \sqrt{\frac{(0.9 - 0.3\epsilon)^2}{4} - 0.05} \right)^{1.67}. \quad (16)$$

In eq. (13) and eq. (15),  $\bar{\lambda}_{p,\theta,0}$  is the threshold plate slenderness and  $\bar{\lambda}_{p,\theta}$  is the elevated temperature plate slenderness calculated as:

$$\bar{\lambda}_{p,\theta} = \xi_\theta \sqrt{\frac{f_y}{\sigma_{cr}}} \quad \text{with} \quad \xi_\theta = \sqrt{\frac{k_{y,\theta}^*}{k_{E,\theta}}}, \quad (17)$$

where  $f_y$  is the room temperature yield strength and  $\sigma_{cr}$  is the elastic critical buckling stress calculated using the following equation:

$$\sigma_{cr} = k_\sigma \frac{\pi^2 E}{12(1 - \nu^2)} \left( \frac{t}{b} \right)^2, \quad (18)$$

in which  $k_\sigma$  is the plate buckling coefficient determined considering the boundary conditions and stress distribution of the plate as described in EN 1993-1-5 [36],  $\nu$  is the Poisson's ratio and  $b$  and  $t$  are the plate width and thickness, respectively.

In the determination of the elevated temperature plate slenderness  $\bar{\lambda}_{p,\theta}$  given by eq. (17),  $k_{y,\theta}^*$  is utilised, which is referred to as the modified elevated temperature yield strength reduction factor herein. The modified elevated temperature yield strength reduction factor  $k_{y,\theta}^*$  is determined as follows:

$$k_{y,\theta}^* = k_{y,\theta} \quad \text{if} \quad k_{\epsilon_{u,\theta}} \epsilon_{u,\theta} \geq 0.02, \quad (19)$$

$$k_{y,\theta}^* = k_{u,\theta} \frac{f_u}{f_y} \quad \text{if} \quad k_{\epsilon_{u,\theta}} \epsilon_{u,\theta} < 0.02. \quad (20)$$

The adoption of the modified elevated temperature yield strength reduction factor  $k_{y,\theta}^*$  in the effective width design equations and in the estimations of the ultimate resistances of steel sections as introduced in the following section obviates the use of the elevated temperature material strength at 2% total strain  $f_{y,\theta} = k_{y,\theta} f_y$  in the cases where the total strains at the attainment of the elevated temperature ultimate strengths  $\epsilon_{u,\theta} = k_{\epsilon_{u,\theta}} \epsilon_u$  are less than 2% (i.e.  $\epsilon_{u,\theta} < 0.02$ ), which was observed for grade S690 and S460 high strengths steels at some elevated temperature levels as illustrated in Fig. 4. This approach avoids the use of the elevated temperature material strengths at 2% total strains  $f_{y,\theta} = k_{y,\theta} f_y$  when they are on the descending branches of the elevated temperature stress-strain curves, enabling the use of the elevated temperature ultimate strengths  $f_{u,\theta} = k_{u,\theta} f_u$  in these cases. In Kucukler [13, 41], this proposed approach was adopted for the ultimate strength predictions of high strength steel circular hollow sections (CHS) and high strength steel plates in fire, where it was shown that the proposed approach leads to accurate resistance predictions for such structural elements at elevated temperatures.

It is worth emphasising that the local buckling assessment equations provided in eqs. (13)-(20) were derived in Kucukler [13] on the basis of a large number of numerical results on the local buckling behaviour of individual normal strength and high strength steel plates in fire. In this study, these equations were adopted for the determination of the ultimate strengths of normal and high strength steel I-sections in fire which undergo local buckling. The accuracy of these equations is assessed for the ultimate strength predictions of normal and high strength steel I-sections undergoing local buckling at elevated temperatures. The peak loads from the finite element analyses of normal and high strength steel I-section in fire obtained from the parametric studies set out in Section 2.5 were used in the assessment of the accuracy of the local buckling assessment equations provided in eqs. (13)-(20).

#### 4.3. Cross-section resistance

Table 7 shows the determination of the elevated temperature ultimate resistances of normal and high strength steel sections falling into the non-slender and slender classes according the design approach proposed in this paper. For cross-sections falling into the non-slender class, it is proposed to use the full cross-section areas  $A$  and the plastic section moduli  $W_{pl}$  in the determination of ultimate resistances, while the use of the effective cross-section areas  $A_{eff}$  and the effective section moduli  $W_{eff}$  is recommended for the ultimate

Table 7: Cross-section resistances of non-slender and slender sections according to the proposed design method

Cross-section class	Design resistance under compression	Design resistance under bending
Non-slender	$N_{fi,t,Rd} = A k_{y,\theta}^* f_y / \gamma_{M,fi}$	$M_{fi,t,Rd} = W_{pl} k_{y,\theta}^* f_y / \gamma_{M,fi}$
Slender	$N_{fi,t,Rd} = A_{eff} k_{y,\theta}^* f_y / \gamma_{M,fi}$	$M_{fi,t,Rd} = W_{eff} k_{y,\theta}^* f_y / \gamma_{M,fi}$

strength predictions of slender cross-sections. Note that the use of eqs. (13) and (15) is recommended for the determination of the effective cross-section areas  $A_{eff}$  and the effective section moduli  $W_{eff}$  in accordance with the procedure provided in EN 1993-1-5 [36]. Similar to proposals made in this study, [9, 22] also recommended the adoption of two cross-section classes in the determination of the ultimate load carrying capacities of steel sections in fire.

As described in the previous subsections, the proposed cross-section classification approach and effective width design equations given by eqs. (13) and (15) adopt the elevated temperature plate slenderness  $\bar{\lambda}_{p,\theta}$  in contrast with EN 1993-1-2 [1] and prEN 1993-1-2 [12] for the design of steel sections in fire. The use of the elevated temperature plate slenderness  $\bar{\lambda}_{p,\theta}$  in the fire design of steel sections enables the consideration of the differential erosions of the strengths  $k_{y,\theta}^*$  and stiffnesses  $k_{E,\theta}$  at different elevated temperature levels on the behaviour, thereby leading to accurate estimations of the ultimate resistances of steel I-sections in fire which will be illustrated in the following sections. However, if the consideration of the differential erosions of the strengths  $k_{y,\theta}^*$  and stiffnesses  $k_{E,\theta}$  at different elevated temperature levels is deemed to lead to an increased complexity in the fire design of steel sections by a designer, the proposed cross-section classification rules and effective width design equations can be made independent of the elevated temperature levels by employing the maximum values of  $\xi_\theta = \max \left( \sqrt{k_{y,\theta}^* / k_{E,\theta}} \right)$  given by the expressions below to determine the elevated temperature plate slendernesses  $\bar{\lambda}_{p,\theta}$  as given by eq. (17):

$$\begin{aligned} \xi_{\theta,const} &= \max \left( \sqrt{k_{y,\theta}^* / k_{E,\theta}} \right) \approx 1.0 \quad \text{for S690 steel,} \\ \xi_{\theta,const} &= \max \left( \sqrt{k_{y,\theta}^* / k_{E,\theta}} \right) \approx 1.2 \quad \text{for S460, S355, S275, S235 steel.} \end{aligned} \quad (21)$$

## 5. Comparison of the accuracy and reliability of the proposed design rules against those of EN 1993-1-2 and prEN 1993-1-2

In this section, the accuracy and reliability of the proposed cross-section design rules are assessed against that of EN 1993-1-2 [1] and prEN 1993-1-2 [12] for the ultimate strength predictions of normal and high strength steel I-sections.

### 5.1. Accuracy assessment

In Figs. 8 and 9, the accuracy of the proposed design rules for the ultimate strength predictions of normal and high strength steel I-sections in compression and major axis bending



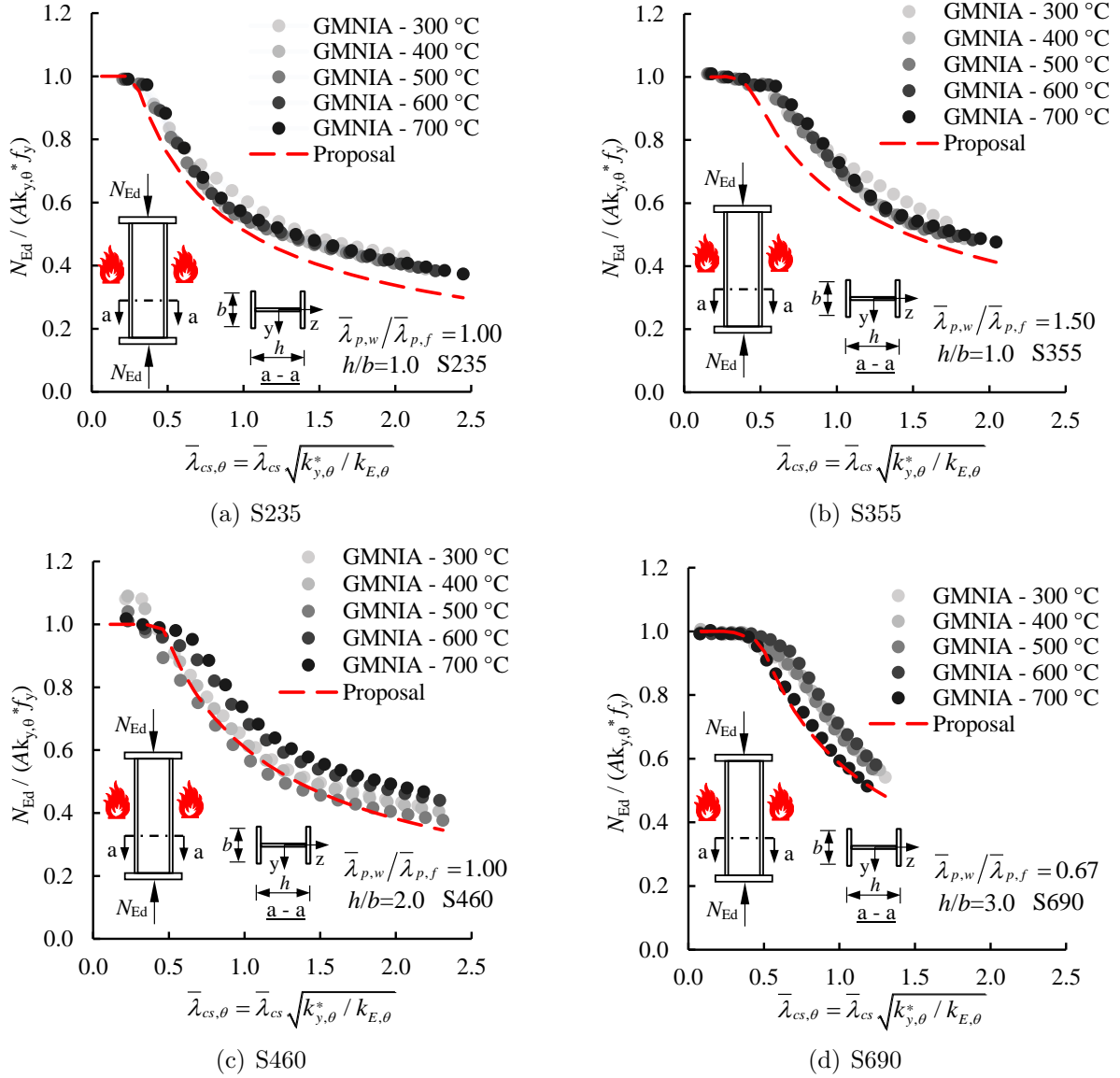


Figure 8: Accuracy of the proposed design rules for the predictions of the ultimate resistances of normal and high strength steel I-sections under compression in fire

in fire is shown, respectively. In the figures,  $\bar{\lambda}_{cs,\theta}$  is the elevated temperature cross-section slenderness determined through the multiplication of the room temperature cross-section slenderness  $\bar{\lambda}_{cs}$  by the square root of the ratio of the modified yield strength reduction factor  $k_{y,\theta}^*$  to the Young's modulus reduction factor  $k_{E,\theta}$  (i.e.  $\bar{\lambda}_{cs,\theta} = \bar{\lambda}_{cs} \sqrt{k_{y,\theta}^* / k_{E,\theta}}$ ). Note that the elevated temperature cross-section slendernesses  $\bar{\lambda}_{cs,\theta}$  are utilised in the illustration of the accuracy of the proposed design rules in Fig. 8 since the proposed cross-section fire design rules use the elevated temperature plate slendernesses  $\bar{\lambda}_{p,\theta} = \bar{\lambda}_p \sqrt{k_{y,\theta}^* / k_{E,\theta}}$  in the determination of the plate buckling reduction factors  $\rho$  employed to determine the effective

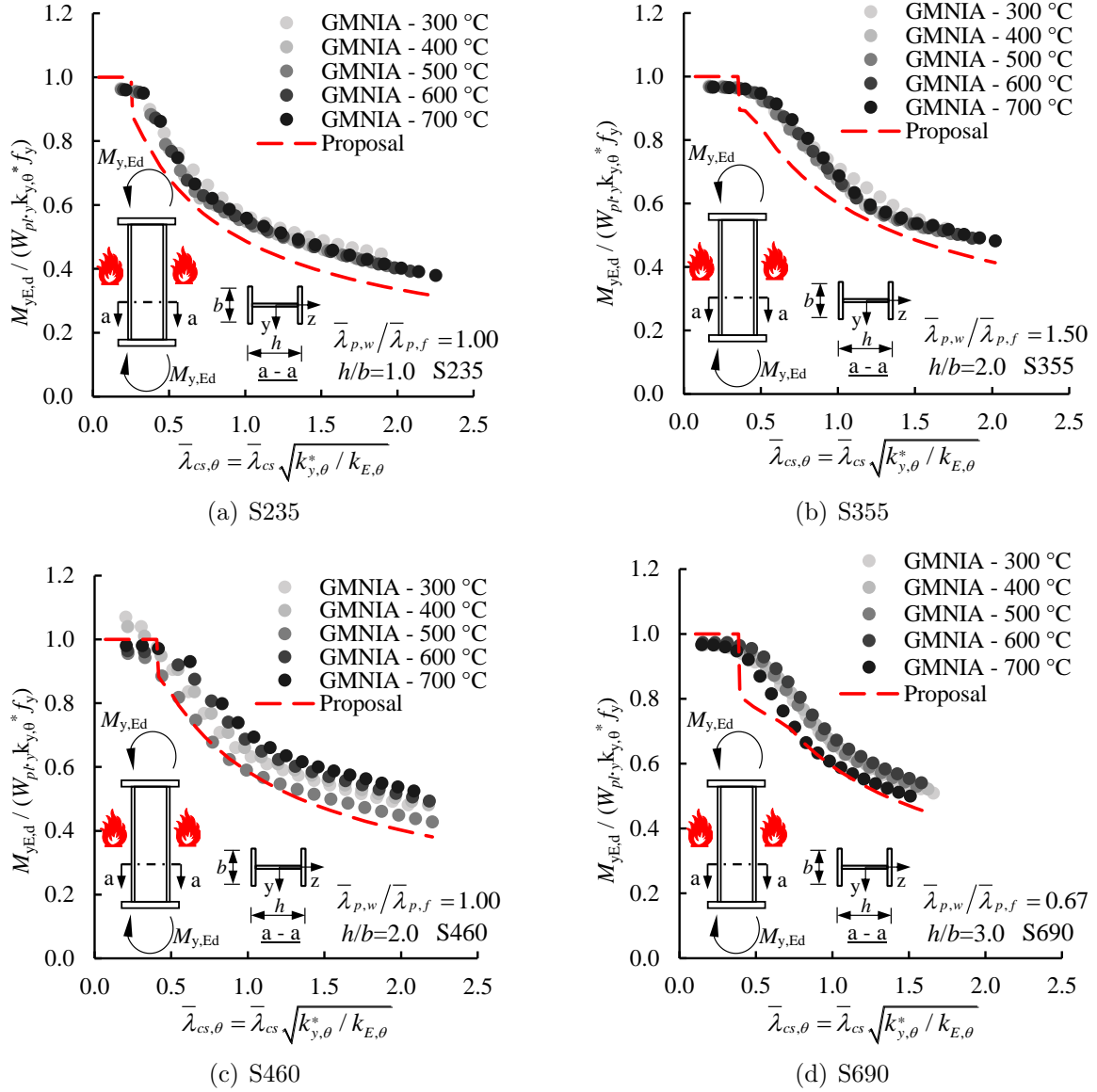


Figure 9: Accuracy of EN 1993-1-2 [1] and prEN 1993-1-2 [12] for the predictions of the ultimate resistances of normal and high strength steel I-sections under bending in fire

cross-section properties (i.e.  $A_{eff}$ ,  $W_{eff}$ ) of cross-sections undergoing local buckling in fire. As can be seen from Figs. 8 and 9, relative to both EN 1993-1-2 [1] and prEN 1993-1-2 [12], the proposed design rules bring about markedly improved accuracy in the ultimate resistance predictions of normal and high strength steel I-sections under compression and major axis bending at elevated temperatures. The markedly increased accuracy of the proposed design rules can be ascribed to the consideration of the differential erosions of the strength and stiffnesses of steel I-sections in fire on the response by means of the elevated temperature plate slendernesses  $\bar{\lambda}_{p,\theta} = \bar{\lambda}_p \sqrt{k_{y,\theta}^* / k_{E,\theta}}$  used in the determination of the effective cross-section

properties (i.e.  $A_{eff}$ ,  $W_{eff}$ ) for cross-sections undergoing local buckling in fire. Moreover, in addition to this, the proposed cross-section design rules in this paper adopt the modified elevated temperature yield strength reduction factor  $k_y^*$  that (i) accounts for the cases where the elevated temperature material strengths at 2% total strains  $f_{y,\theta} = k_{y,\theta} f_y$  are on the descending branches of the elevated temperature stress-strain curves of high strength steels and (ii) enables the use of the elevated temperature ultimate material strengths  $f_{u,\theta} = k_{u,\theta} f_u$  instead, as described in Section 5.2. Figs. 8 and 9 show that the adoption of the modified elevated temperature yield strength reduction factor  $k_y^*$  to determine the elevated temperature material strengths  $f_{y,\theta} = k_{y,\theta}^* f_y$  lead to significantly improved accuracy for the ultimate strength predictions of grade S690 and S460 steel I-sections in fire relative to EN 1993-1-2 [1] and prEN 1993-1-2 [12] whose accuracy is illustrated in Figs. 6 and 7.

A comparison of the accuracy of the proposed design rules against the accuracy of EN 1993-1-2 [1] and prEN 1993-1-2 [12] is shown in Table 8 and Fig. 10, taking into account

Table 8: Assessment of the accuracy of the proposed design rules and those provided in EN 1993-1-2 [1] and prEN 1993-1-2 [12] for the ultimate strength predictions of high strength and normal strength steel I-sections in fire

Design method	Steel grade	N	$\zeta_{av}$	$\zeta_{COV}$	$\zeta_{max}$	$\zeta_{min}$
Proposal	S690	2850	1.10	0.093	1.50	0.90
	S460	2850	1.13	0.099	1.55	0.90
	S355	2850	1.11	0.086	1.53	0.94
	S275	2850	1.14	0.105	1.62	0.94
	S235	2850	1.16	0.097	1.68	0.95
Simplified proposal with constant $\xi_\theta$	S690	2850	1.14	0.128	1.72	0.91
	S460	2850	1.15	0.111	1.70	0.90
	S355	2850	1.11	0.091	1.54	0.92
	S275	2850	1.14	0.116	1.66	0.94
	S235	2850	1.16	0.104	1.71	0.95
prEN 1993-1-2 [12]	S690	2850	1.19	0.141	1.81	0.83
	S460	2850	1.17	0.146	2.34	0.69
	S355	2850	1.12	0.129	1.61	0.76
	S275	2850	1.13	0.148	1.84	0.73
	S235	2850	1.12	0.140	1.64	0.71
EN 1993-1-2 [1]	S690	2850	1.11	0.112	1.72	0.90
	S460	2850	1.11	0.146	1.78	0.75
	S355	2850	1.19	0.187	2.10	0.68
	S275	2850	1.16	0.197	2.06	0.64
	S235	2850	1.13	0.187	2.05	0.61

the broad range of parameters provided in Table 4. In Table 8 and Fig. 10,  $\zeta$  is the ratio of the ultimate load carrying capacity of a steel section obtained from the GMNIA  $R_{GMNIA}$  to that determined through a design method  $R_{method}$  (i.e.  $\zeta = R_{GMNIA}/R_{method}$ ) and  $\zeta_{av}$ ,  $\zeta_{COV}$ ,  $\zeta_{max}$  and  $\zeta_{min}$  are the average, coefficient of variation, maximum and minimum of  $\zeta$  values, respectively. Note that a  $\zeta$  value less than 1.0 (i.e.  $\zeta < 1.0$ ) indicates that a method

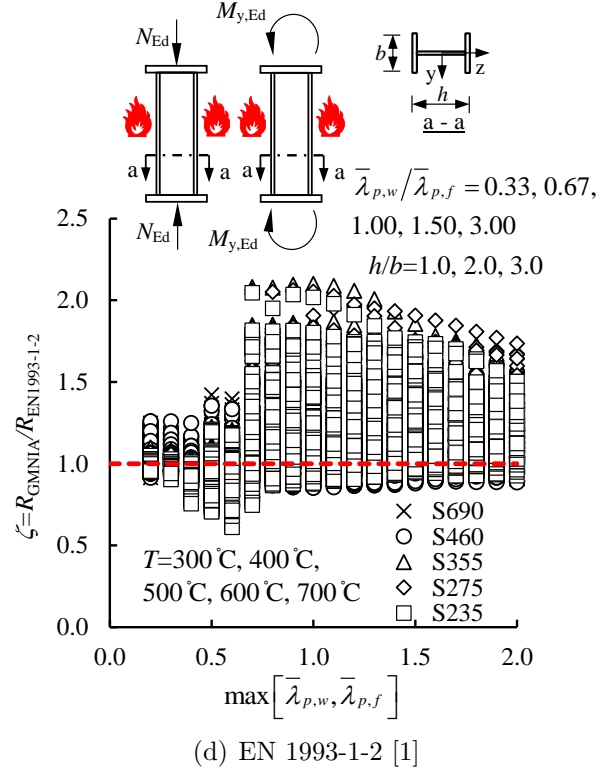
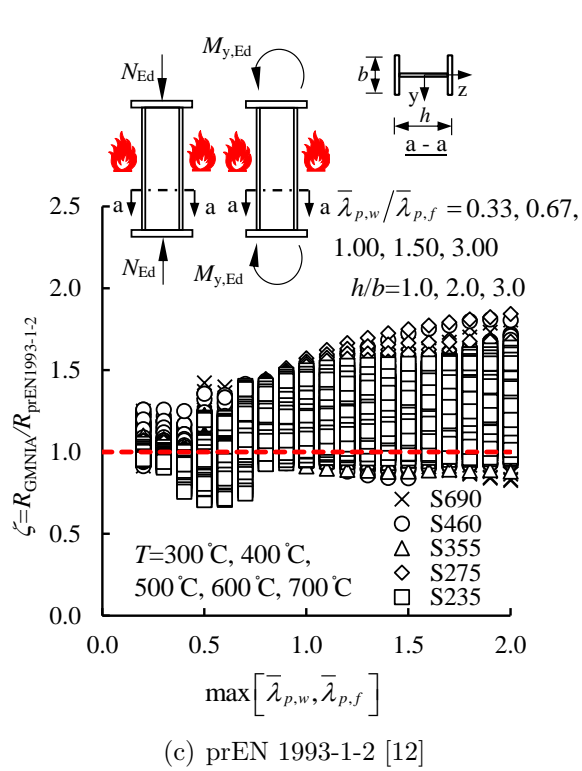
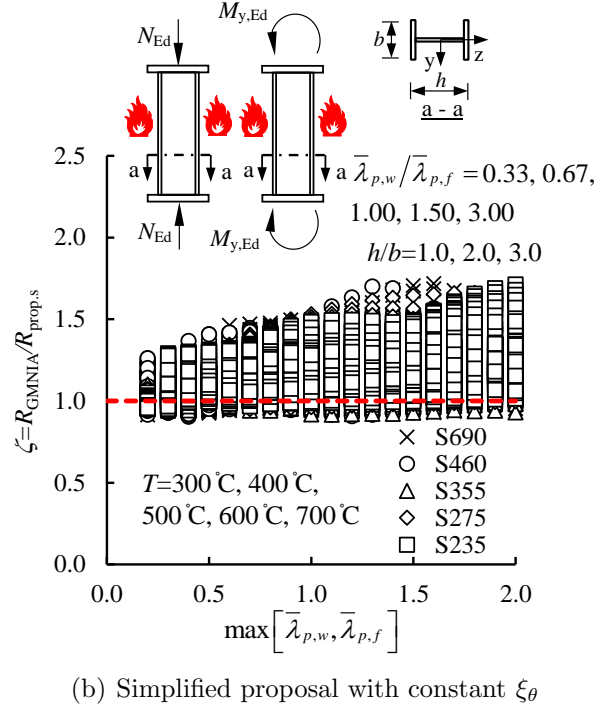
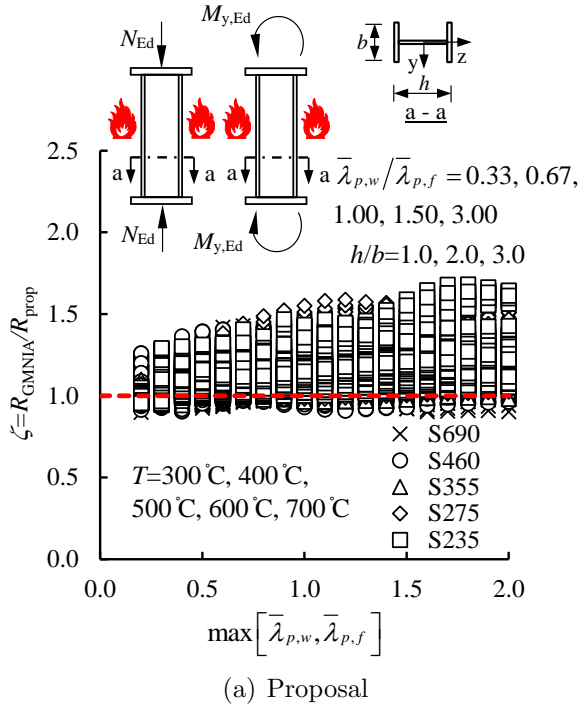


Figure 10: Accuracy of the proposed design rules for the predictions of the ultimate resistances of normal and high strength steel I-sections under compression in fire

is unsafe and the ultimate resistances obtained from a design method  $R_{method}$  are denoted by  $R_{prop}$ ,  $R_{EN1993-1-2}$  and  $R_{prEN1993-1-2}$  for the proposed design rules, EN 1993-1-2 [1] and prEN 1993-1-2 [12], respectively. Table 8 and Fig. 10 show that the proposed design rules in this paper lead to more accurate ultimate cross-section strength predictions relative to both EN 1993-1-2 [1] and prEN 1993-1-2 [12] for grade S355, S275 and S235 normal strength and grade S690 and S460 high strength steel I-sections in fire, considering the very broad range of parameters summarised in Table 4.

As indicated in Section 5.3, the proposed cross-section design rules in this paper can be applied using constant  $\zeta_{\theta,const}$  factors given by eq. (21) which makes the proposed cross-section classification rules and effective width design equations independent of the elevated temperature levels, thereby simplifying the proposed design procedure if it is deemed preferable by a designer. The accuracy of the simplified version of the proposed cross-section design rules applied with the adoption of the constant  $\zeta_{\theta,const}$  factors given by eq. (21) is also compared against the accuracy of EN 1993-1-2 [1] and prEN 1993-1-2 [12] in Table 8 and Fig. 10 for the ultimate resistance predictions of normal and high strength steel I-sections at elevated temperatures. As can be seen from Table 8 and Fig. 10, the proposed design rules also lead to more accurate ultimate strength predictions for normal and high strength steel I-sections in fire relative to EN 1993-1-2 [1] and prEN 1993-1-2 [12] when they are applied using constant  $\zeta_{\theta,const}$  factors given by eq. (21), so verifying the appropriateness of the simplified version of the proposed cross-section fire design rules for normal and high strength steel I-sections if they are found preferable by a designer.

## 5.2. Reliability assessment

In this subsection, the reliability of the proposed design rules in this paper and that of EN 1993-1-2 [1] and prEN 1993-1-2 [12] are assessed for the cross-section design of normal and high strength steel I-sections at elevated temperatures, adopting the three reliability criteria proposed by Kruppa [44] for the fire design methods of structural steel elements. The Criterion 1 of Kruppa [44] states that none of the ultimate resistance estimations obtained from a design method  $R_{method}$  should exceed those determined through the GMNIA of the finite element models  $R_{GMNIA}$  by more than 15%, i.e.  $(R_{method} - R_{GMNIA})/R_{GMNIA} \leq 15\%$ . According to the Criterion 2 of [44], less than 20% of the design predictions should be on the unsafe side, i.e.  $num(R_{method} > R_{GMNIA})/num(R_{method}) \leq 20\%$ . The Criterion 3 of [44] requires that the design estimations have to be safe-sided on average, i.e.  $\bar{X}[(R_{method} - R_{GMNIA})/R_{GMNIA}] \leq 0\%$ . Table 9 shows the reliability of the proposed cross-section design rules, their simplified version when they are applied with constant  $\zeta_{\theta,const}$  given by eq. (21), prEN 1993-1-2 [12] and EN 1993-1-2 [1]. Note that in the table, the percentage of the cases where the resistances determined by a design method exceed those determined through the GMNIA by more than 15% are shown under Criterion 1, the percentage of the cases where the resistances are overestimated are displayed under Criterion 2 and the average percentage differences between the design predictions and the GMNIA results are shown under Criterion 3 where the negative values signify that the design predictions are safe-sided on average. In Table 9, the violated criteria are marked with ‘\*’. As can be seen from Table 9, the proposed design rules satisfy all the three reliability criteria of Kruppa [44]

Table 9: Assessment of the reliability of the proposed design rules and those provided in EN 1993-1-2 [1] and prEN 1993-1-2 [12] for the ultimate strength predictions of high strength and normal strength steel I-sections in fire on the basis of the reliability criteria set out by Kruppa [44]. Note that a number denoted by \* violates the corresponding criterion

Design method	Steel grade	Criterion 1	Criterion 2	Criterion 3
Proposal	S690	0.00	18.69	-8.48
	S460	0.00	10.50	-11.50
	S355	0.00	11.06	-9.28
	S275	0.00	8.28	-11.44
	S235	0.00	6.12	-12.72
Simplified proposal with constant $\xi_\theta$	S690	0.00	16.53	-10.97
	S460	0.00	9.79	-12.20
	S355	0.00	13.48	-9.09
	S275	0.00	10.03	-11.16
	S235	0.00	6.97	-12.59
prEN 1993-1-2 [12]	S690	0.21*	10.26	-14.35
	S460	0.50*	15.11	-12.70
	S355	1.64*	23.61*	-9.11
	S275	2.87*	22.42*	-9.62
	S235	4.21*	23.67*	-9.07
EN 1993-1-2 [1]	S690	0.00	14.71	-9.14
	S460	1.35*	25.07*	-8.37
	S355	2.32*	23.89*	-13.24
	S275	3.61*	28.22*	-10.87
	S235	5.06*	32.52*	-8.76

for grade S355, S275 and S235 normal strength and grade S690 and S460 high strength steel I-sections subjected to pure compression and pure major axis bending in fire, considering the broad range of parameters corresponding to 14250 cross-sections which are summarised in Table 4. On the other hand both EN 1993-1-2 [1] and pr EN 1993-1-2 [12] violate the Criterion 1 and Criterion 2 of Kruppa [44] for a high number of cases, highlighting that the cross-section fire design rules proposed in this paper lead to more reliable ultimate resistance predictions for normal and high strength steel I-sections in fire. Table 9 also illustrate that the simplified version of the proposed cross-section design rules applied with the constant  $\zeta_{\theta, const}$  also satisfy all the three reliability criteria of [44] for all the considered cases, so indicating that the simplified version of the proposed design rules also lead to reliable capacity predictions if they are preferred by a designer for the design of normal and high strength steel I-sections in fire.

## 6. Conclusions

In this study, the behaviour and design of grade S690 and S460 high strength steel and grade S355, S275 and S235 normal strength steel I-sections at elevated temperatures were investigated. Finite element models of high strength steel and normal strength steel I-sections

able to replicate their structural response in fire were created and validated against experimental data from fire tests on steel I-sections in the literature. Through the validated finite element models of normal and high strength steel I-sections, extensive numerical studies were performed, taking into account different cross-section aspect ratios, elevated temperature levels, S690 and S460 high strength grades and S355, S275 and S235 normal strength steel grades and various plate slendernesses for constituent cross-section elements (i.e. web and flange plates). The structural performance data obtained from the nonlinear shell finite element modelling were used to assess the accuracy of EN 1993-1-2 [1], prEN 1993-1-2 [12] and proposed cross-section fire design rules for normal and high strength steel I-sections at elevated temperatures. In the following, the key findings and primary contributions of this study are set out:

- This study found that the European structural steel fire design standard EN 1993-1-2 [1] and its upcoming version prEN 1993-1-2 [12] can provide somewhat inaccurate ultimate strength predictions for normal and high strength steel I-sections in fire.
- With the aim of accurately estimating the ultimate resistances of normal and high strength steel I-sections at elevated temperatures, new cross-section design rules for normal and high strength steel I-sections in fire based on the proposals of Kucukler [13] for the design of individual steel plates at elevated temperatures are put forward.
- The cross-section design rules proposed for normal and high strength steel I-sections in fire adopt the von Karman effective width concept [45, 46] and cross-section classification approach; thus, they are compatible with the EN 1993-1-2 [1] and prEN 1993-1-2 [12] cross-section design rules.
- Through the use of the elevated temperature plate slenderness  $\bar{\lambda}_{p,\theta} = \bar{\lambda}_p \sqrt{k_{y,\theta}/k_{E,\theta}}$ , the proposed cross-section fire design rules for normal and high strength steel I-sections are able to account for the differential erosions of the strength and stiffness of steel sections at elevated temperatures, which was shown to considerably influence the response in this paper. The EN 1993-1-2 [1] and prEN 1993-1-2 [12] cross-section design rules, on the other hand, do not consider this important effect, adopting the room temperature plate slenderness  $\bar{\lambda}_p$ .
- It was demonstrated that relative to EN 1993-1-2 [1] and prEN 1993-1-2 [12], the proposed cross-section fire design rules in this paper are able to provide more accurate ultimate resistance predictions of grade S690 and S460 high strength and grade S355, S275 and S235 normal strength steel I-sections in fire.
- The proposed cross-section design rules satisfy all the reliability criteria of Kruppa [44] adopted for the reliability assessment of the fire design methods developed for steel structures. On the other hand, EN 1993-1-2 [1] and prEN 1993-1-2 [12] violate the reliability criteria of Kruppa [44]. This finding shows that the proposed cross-section fire design rules in this paper lead to more reliable ultimate strength estimations of

normal and high strength steel I-sections in fire relative to EN 1993-1-2 [1] and prEN 1993-1-2 [12].

## References

- [1] EN 1993-1-2, Eurocode 3 Design of steel structures-Part 1-2: General rules – Structural fire design. European Committee for Standardization (CEN), Brussels; 2005.
- [2] AISC 360-16, Specifications for structural steel buildings. American Institute of Steel Construction (AISC), Chicago; 2016.
- [3] Ranby, A.. Structural fire design of thin walled steel sections. *Journal of Constructional Steel Research* 1998;1(46):303–304.
- [4] Knobloch, M., Fontana, M.. Strain-based approach to local buckling of steel sections subjected to fire. *Journal of constructional steel research* 2006;62(1-2):44–67.
- [5] Heidarpour, A., Bradford, M.A.. Local buckling and slenderness limits for steel webs under combined bending, compression and shear at elevated temperatures. *Thin-Walled structures* 2008;46(2):128–146.
- [6] Quiel, S.E., Garlock, M.E.. Calculating the buckling strength of steel plates exposed to fire. *Thin-Walled Structures* 2010;48(9):684–695.
- [7] Selamet, S., Garlock, M.E.. Plate buckling strength of steel wide-flange sections at elevated temperatures. *Journal of Structural Engineering, ASCE* 2013;139(11):1853–1865.
- [8] Couto, C., Real, P.V., Lopes, N., Zhao, B.. Effective width method to account for the local buckling of steel thin plates at elevated temperatures. *Thin-Walled Structures* 2014;84:134–149.
- [9] Couto, C., Real, P.V., Lopes, N., Zhao, B.. Resistance of steel cross-sections with local buckling at elevated temperatures. *Journal of Constructional Steel Research* 2015;109:101–114.
- [10] Theofanous, M., Prossert, T., Knobloch, M., Gardner, L.. The continuous strength method for steel cross-section design at elevated temperatures. *Thin-Walled Structures* 2016;98:94–102.
- [11] ENV 1993-1-1, Eurocode 3 Design of steel structures-Part 1-1: General rules and rules for buildings. European Committee for Standardization (CEN), Brussels; 1992.
- [12] prEN 1993-1-2, Final Draft of EN 1993-1-2, Eurocode 3 Design of steel structures-Part 1-2: General rules – Structural fire design. European Committee for Standardization (CEN), Brussels; 2019.
- [13] Kucukler, M.. Local stability of normal and high strength steel plates at elevated temperatures. *Engineering Structures* 2021;243:112528.
- [14] Bambach, M.R., Rasmussen, K.J.. Effective widths of unstiffened elements with stress gradient. *Journal of Structural Engineering, ASCE* 2004;130(10):1611–1619.
- [15] Xing, Z., Kucukler, M., Gardner, L.. Local buckling of stainless steel I-sections in fire: Finite element modelling and design. *Thin-Walled Structures* 2021;161:107486.
- [16] Abaqus 2018 Reference Manual. Simulia, Dassault Systemes; 2018.
- [17] Kucukler, M., Gardner, L., Macorini, L.. Lateral-torsional buckling assessment of steel beams through a stiffness reduction method. *Journal of Constructional Steel Research* 2015;109:87–100.
- [18] Kucukler, M., Gardner, L., Macorini, L.. Flexural-torsional buckling assessment of steel beam-columns through a stiffness reduction method. *Engineering Structures* 2015;101:662–676.
- [19] Kucukler, M., Gardner, L.. Design of web-tapered steel beams against lateral-torsional buckling through a stiffness reduction method. *Engineering Structures* 2019;190:246–261.
- [20] Kucukler, M., Xing, Z., Gardner, L.. Behaviour and design of stainless steel I-section columns in fire. *Journal of Constructional Steel Research* 2020;165:105890.
- [21] Kucukler, M.. Lateral instability of steel beams in fire: Behaviour, numerical modelling and design. *Journal of Constructional Steel Research* 2020;170:106095.
- [22] Xing, Z., Kucukler, M., Gardner, L.. Local buckling of stainless steel plates in fire. *Thin-Walled Structures* 2020;148:106570.
- [23] Ziemian, R.D.. Guide to stability design criteria for metal structures. John Wiley & Sons; 2010.
- [24] Crisfield, M.A.. A fast incremental/iterative solution procedure that handles “snap-through”. *Computers & Structures* 1981;13(1-3):55–62.



- [25] Ramm, E.. Strategies for tracing the nonlinear response near limit points. In: Nonlinear finite element analysis in structural mechanics. Springer; 1981, p. 63–89.
- [26] Rubert, A., Schaumann, P.. Structural steel and plane frame assemblies under fire action. *Fire Safety Journal* 1986;10(3):173–184.
- [27] Schneider, R., Lange, J.. Constitutive equations of structural steel S460 at high temperatures. In: Nordic Steel Construction Conference Proceedings, Malmo, Sweden. 2009, p. 204–211.
- [28] Choi, I.R., Chung, K.S., Kim, D.H.. Thermal and mechanical properties of high-strength structural steel HSA800 at elevated temperatures. *Materials & Design* 2014;63:544–551.
- [29] Xiong, M.X., Liew, J.R.. Mechanical properties of heat-treated high tensile structural steel at elevated temperatures. *Thin-Walled Structures* 2016;98:169–176.
- [30] Fang, H., Chan, T.M.. Axial compressive strength of welded S460 steel columns at elevated temperatures. *Thin-walled Structures* 2018;129:213–224.
- [31] Fang, H., Chan, T.M.. Resistance of axially loaded hot-finished S460 and S690 steel square hollow stub columns at elevated temperatures. *Structures* 2019;17:66–73.
- [32] Chen, J., Young, B.. Design of high strength steel columns at elevated temperatures. *Journal of Constructional Steel Research* 2008;64(6):689–703.
- [33] Mirambell, E., Real, E.. On the calculation of deflections in structural stainless steel beams: An experimental and numerical investigation. *Journal of Constructional Steel Research* 2000;54(1):109–133.
- [34] Qiang, X., Bijlaard, F., Kolstein, H.. Dependence of mechanical properties of high strength steel S690 on elevated temperatures. *Construction and Building Materials* 2012;30:73–79.
- [35] Qiang, X., Bijlaard, F.S., Kolstein, H.. Elevated-temperature mechanical properties of high strength structural steel S460N: Experimental study and recommendations for fire-resistance design. *Fire Safety Journal* 2013;55:15–21.
- [36] EN 1993-1-5, Eurocode 3 Design of steel structures-Part 1-5: Plated structural elements. European Committee for Standardization (CEN), Brussels; 2005.
- [37] Wang, W., Kodur, V., Yang, X., Li, G.. Experimental study on local buckling of axially compressed steel stub columns at elevated temperatures. *Thin-Walled Structures* 2014;82:33–45.
- [38] Sharhan, A., Wang, W., Li, X., Al-azzani, H.. Steady and transient state tests on local buckling of high strength Q690 steel stub columns. *Thin-Walled Structures* 2021;167:108214.
- [39] ECCS, Ultimate limit state calculation of sway frames with rigid joints. Tech. Rep.; No. 33, Technical Committee 8 (TC 8) of European Convention for Constructional Steelwork (ECCS); 1984.
- [40] Bradford, M.A., Liu, X.. Flexural-torsional buckling of high-strength steel beams. *Journal of Constructional Steel Research* 2016;124:122–131.
- [41] Kucukler, M.. Compressive resistance of high-strength and normal-strength steel CHS members at elevated temperatures. *Thin-Walled Structures* 2020;152:106753.
- [42] EN 1993-1-1, Eurocode 3 Design of steel structures-Part 1-1: General rules and rules for buildings. European Committee for Standardization (CEN), Brussels; 2005.
- [43] prEN 1993-1-1, Final Draft of Eurocode 3 Design of steel structures-Part 1-1: General rules and rules for buildings. European Committee for Standardization (CEN), Brussels; 2018.
- [44] Kruppa, J.. Eurocodes–Fire parts: Proposal for a methodology to check the accuracy of assessment methods. CEN TC 250, Horizontal Group Fire, Document no: 99/130; 1999.
- [45] Von Kármán, T.. The strength of thin plates in compression. *Trans ASME* 1932;54:53–57.
- [46] Winter, G.. Strength of thin steel compression flanges. *Transactions of the American Society of Civil Engineers* 1947;112(1):527–554.